Neurobiology of Disease 36 (2009) 126–141

Contents lists available at ScienceDirect

Neurobiology of Disease

journal homepage: www.elsevier.com/locate/ynbdi

A role for the preoptic sleep-promoting system in absence epilepsy

N. Suntsova [a,b,e,*], S. Kumar [a,c,f], R. Guzman-Marin [d], M.N. Alam [a,b], R. Szymusiak [a,c], D. McGinty [a,b,*]

[a] Research Service, Veterans Affairs Greater Los Angeles Healthcare System, North Hills, CA 91343, USA
[b] Department of Psychology, University of California Los Angeles, Los Angeles, CA 90095, USA
[c] Department of Medicine, University of California Los Angeles, Los Angeles, CA 90095, USA
[d] Department of Neurology, University of California Los Angeles, Los Angeles, CA 90095, USA
[e] A.B. Kogan Research Institute for Neurocybernetics, Southern Federal University, Rostov-on-Don, 344091, Russia
[f] Department of Zoology, Patna University, Patna, India

ARTICLE INFO

Article history:
Received 3 April 2009
Revised 26 June 2009
Accepted 13 July 2009
Available online 23 July 2009

Keywords:
Absence epilepsy
Spike-wave discharges
Sleep
Median preoptic nucleus
Ventrolateral preoptic nucleus
GABAergic neurons
c-Fos
Neuronal activity
WAG/Rij rats

ABSTRACT

Absence epilepsy (AE) in humans and the genetic AE model in WAG/Rij rats are both associated with abnormalities in sleep architecture that suggest insufficiency of the sleep-promoting mechanisms. In this study we compared the functionality of sleep-active neuronal groups within two well-established sleep-promoting sites, the ventrolateral and median preoptic nuclei (VLPO and MnPN, respectively), in WAG/Rij and control rats. Neuronal activity was assessed using c-Fos immunoreactivity and chronic single-unit recording techniques. We found that WAG/Rij rats exhibited a lack of sleep-associated c-Fos activation of GABAergic MnPN and VLPO neurons, a lower percentage of MnPN and VLPO cells increasing discharge during sleep and reduced firing rates of MnPN sleep-active neurons, compared to non-epileptic rats. The role of sleep-promoting mechanisms in pathogenesis of absence seizures was assessed in non-epileptic rats using electrical stimulation and chemical manipulations restricted to the MnPN. We found that fractional activation of the sleep-promoting system in waking was sufficient to elicit absence-like seizures. Given that reciprocally interrelated sleep-promoting and arousal neuronal groups control thalamocortical excitability, we hypothesize that malfunctioning of sleep-promoting system results in impaired ascending control over thalamocortical rhythmogenic mechanisms during wake–sleep transitions thus favoring aberrant thalamocortical oscillations. Our findings suggest a pathological basis for AE-associated sleep abnormalities and a mechanism underlying association of absence seizures with wake–sleep transitions.

Published by Elsevier Inc.

Introduction

The sleep–waking cycle is a key factor influencing the expression of absence epilepsy (AE). EEG hallmarks of absence seizures, spike-wave discharges (SWDs), are strongly inhibited during alert wakefulness and rapid eye movement (REM) sleep and predominantly occur during transitory decreases in the level of vigilance in wakefulness, during light non-REM sleep (NREM) and transitions from NREM to REM sleep (Halasz et al., 2002). AE and other forms of idiopathic generalized epilepsy are associated with a number of abnormalities in sleep architecture including longer latencies to sleep and REM sleep onset, increased percentage of drowsiness and awakenings, reduced REM sleep percentage and decreased sleep efficiency (Baldy-Moulinier, 1992; Barreto et al., 2002; Maganti et al., 2005; Sun et al., 2005; Huang et al., 2007). AE patients also have increased daytime somnolence (Maganti et al., 2006, Byars et al., 2008). Similar changes in sleep parameters were found in Wistar Albino Glaxo/Rijswijk (WAG/Rij) rats, an accepted genetic model of human absence epilepsy, including prolonged transitional periods from wakefulness to sleep, lengthened intermediate stage of sleep, more frequently followed by arousals, and decreased REM sleep percentage (Gandolfo et al., 1990; Coenen and van Luijtelaar, 2003; van Luijtelaar and Bikbaev, 2007). These changes in sleep architecture suggest a hypothesis that AE is associated with insufficiency of the sleep-promoting mechanisms. Neuronal groups putatively involved in sleep initiation and maintenance via inhibitory control over multiple arousal neuronal groups were identified within two preoptic area subregions, the ventrolateral preoptic area (VLPO) and the median preoptic nucleus (MnPN) (Sherin et al., 1996; Gong et al., 2000). Malfunctioning of the preoptic sleep-promoting neuronal populations may be implicated in the mechanisms associating SWDs with transitional periods from wakefulness to sleep.

Like rhythms typical of normal NREM sleep, SWDs are generated within the thalamocortical circuitry (Crunelli and Leresche, 2002; Huguenard and McCormick, 2007). Aberrant thalamocortical oscillations may result from excessive neocortical excitability (Gloor and Fariello, 1988) and/or increased thalamic synchronization (Huguenard and McCormick, 2007) caused by impaired neurotransmission (Pumain et al., 1992; Avanzini et al., 1996; Luhmann et al., 1995;

* Corresponding authors. Research Service (151A3), V.A. Greater Los Angeles, Healthcare System, 16111 Plummer St., North Hills, CA, 91343, USA. Fax: +1 818 985 9575.
E-mail addresses: suntsova@ucla.edu (N. Suntsova), dmcginty@ucla.edu (D. McGinty).
Available online on ScienceDirect (www.sciencedirect.com).

0969-9961/$ – see front matter. Published by Elsevier Inc.
doi:10.1016/j.nbd.2009.07.005

Hosford et al., 1997; D'Antuono et al. 2006; Merlo et al., 2007; Tan et al., 2008) and/or dysfunctional ion channels (Crunelli and Leresche, 2002; Talley et al., 2000; Budde et al., 2005; Strauss et al., 2004; Kole et al., 2007; Broicher et al., 2008). However, thalamocortical rhythmogenic mechanisms are highly controlled by cholinergic, monoaminergic and hypocretinergic/orexinergic neuronal groups, which affect both excitability and firing mode of thalamocortical cells by modulation of the membrane and synaptic properties of neurons involved in rhythmogenesis (McCormick, 1992; Steriade, 1999; Govindaiah and Cox, 2006). Imbalance in the ascending control of the thalamocortical circuits caused by pathological impairments within multiple arousal system has been suggested as one of the mechanisms underlying SWDs generation (Snead, 1995; Danober et al., 1998). However, arousal neuronal groups are under inhibitory control from the preoptic sleep-active neuronal groups (Saper et al., 2001; Szymusiak and McGinty, 2008). Therefore, imbalance in the ascending control of the thalamocortical circuit may result from abnormal functioning of preoptic sleep-promoting neuronal groups.

The aims of this study were (1) to assess functionality of preoptic sleep-promoting neuronal groups in WAG/Rij rats via comparison of sleep- and wake-related c-Fos protein expression and neuronal discharge within the VLPO and MnPN in WAG/Rij and control non-epileptic rats; (2) to study EEG and behavioral effects of interventions simulating incomplete activation of the sleep-promoting mechanisms in non-epileptic rats. The results demonstrate (1) insufficiency of the sleep-promoting mechanisms in genetically epilepsy-prone rats and (2) induction of absence seizures in response to incomplete activation of the sleep-promoting mechanisms during waking using electrical stimulation and chemical manipulations restricted to the MnPN. We hypothesize that insufficiency of the sleep-promoting system results in abnormal ascending control over thalamocortical excitability during transitions from wakefulness to sleep, favoring aberrant thalamocortical oscillations.

Methods

All experiments were performed in accordance with the National Research Council Guide for the Care and Use of Laboratory Animals. Animal use protocols were reviewed and approved by the Internal Animal Care and Use Committee of the Veterans Affairs Greater Los Angeles Healthcare System.

Animals and experimental environment

Six month old WAG/Rij rats ($n=35$; Harlan, the Netherlands), age-matched Wistar ($n=12$) and August Copenhagen Irish (ACI, $n=12$) control rats (Harlan Sprague Dawley, Indianapolis, IN) were used in this study. At this age absence-like seizures in WAG/Rij rats are fully developed and all animals exhibit hundreds of SWDs/day (Coenen and van Luijtelaar, 2003; van Luijtelaar and Sitnikova, 2006). Less epilepsy-prone outbred Wistar rats (the strain of origin for the inbred WAG/Rij strain) and inbred ACI rats, virtually free of SWDs (Inoue et al., 1990) are commonly used as non-epileptic control animals (Strauss et al., 2004; van de Bovenkamp-Janssen et al., 2004). EEG and behavioral effects of electrical stimulation and chemical manipulations of the MnPN neuronal activity were studied in 6 three month old Sprague–Dawley rats that did not exhibit SWDs during 24 h baseline recordings.

Rats were housed individually in Plexiglas cages or in Stand-alone Raturn Animal Handling System (Bioanalytical Systems, Inc., West Lafayette IN, USA) placed inside an electrically shielded, sound-attenuated chamber. Ambient temperature was maintained at 23 ± 0.5 °C. Rats were kept in a 12 h light/dark cycle with lights on at 7:00 A.M. designated as Zeitgeber time 0 (ZT0). Animals had *ad libitum* access to food and water.

Surgery

Surgical procedures were performed under ketamine/xylazine anesthesia (80/10 mg/kg, *i.p.* respectively) and aseptic conditions.

All rats were surgically prepared for behavioral state assessment and seizure monitoring. Four stainless-steel screw EEG electrodes were placed into the skull symmetrically over the frontal (AP, +2.5; ML, 2.5) and parietal (AP, −2.5, ML, 2.5) cortex. One screw placed in the cranium over the cerebellum served as reference electrode. Four Teflon-coated stainless-steel EMG wires were implanted into the dorsal neck muscles.

To record single-unit activity within the VLPO or the MnPN, a preassembled electrode array was used. It consisted of 10 Formvar-insulated stainless-steel microwires (20 μm) inserted into the 23-gauge guide cannula that was attached to a mechanical microdrive anchored to the miniature electrical connector. The stereotaxic coordinates for the MnPN and VLPO were, respectively: anterioposterior (AP), −0.3; mediolateral (ML), 0; horizontal (H), 6–8 and AP, −0.3; ML, 1; H, 8.5–9.5 (Paxinos and Watson, 1998). The guide cannula was lowered inside the brain to position its tip 3 mm above the target. After fixation of the entire assembly to the skull, the microwires were advanced through the guide cannula to a point corresponding to the dorsal margin of VLPO or MnPN.

To manipulate the MnPN activity, animals were implanted with parallel bipolar Formvar-insulated tungsten electrodes (80 μm, 10–20 kΩ at 1000 Hz) or a guide cannula for subsequent insertion of microdialysis probe as described in detail elsewhere (Suntsova et al., 2007). Briefly, electrode wires targeted the most rostrovental and dorsocaudal portions of the MnPN (*AP*, 0.0; *H*, 7.0 and *AP*, −0.46; *H*, 5, respectively (Swanson, 1998)) to provide stimulation of the entire structure. The guide cannulas were implanted in the midline at a 15° angle from the vertical with tips located 3 mm from the target (*AP*, +0.12; *ML*, 0; *H*, 7.1).

Recording

The rats were allowed to recover from surgery for at least one week, and then were connected to amplifiers through light cables suspended by an overhead counterbalanced cable and slip ring to acclimate them to experimental conditions for 5 days.

Experiments were performed on freely moving animals. EEG and EMG signals were recorded bipolarly using Polygraph model 78 amplifiers (Grass Instruments, Quincy, MA). Passbands were set at 1–30 and 100–1000 Hz, respectively. Neuronal activity was recorded extracellularly using bipolar derivations from microwires (impedance at 1 kHz, 600–750 kΩ). Signals from microwires were first amplified through a miniature headstage preamplifier (MPA-8-I, Multi Channel Systems, Reutlingen, Germany) connected to a differential AC amplifier (model 1700; A-M Systems, Carlsborg, WA) with low and high cutoff filters of 10 Hz and 10 kHz, respectively.

Bioelectrical signals were digitized and stored on hard drive for off-line analysis using Micro 1401 data acquisition interface and Spike2 software package (Cambridge Electronic Design, London, UK). Polygraphic data were digitized at a 256 Hz sampling rate and unit activity data at 10 or 25 kHz for waveform and wavemark data channels, respectively.

Electrical stimulation and reverse microdialysis

Electrical stimulation of the MnPN was performed with 200 μs constant-current square pulses using A-65 Timer/stimulator coupled with SC-100 constant-current monophasic stimulus isolation unit (Winston Electronics Company, USA).

MnPN cellular activity was manipulated using microdialytic application of L-glutamate, the $GABA_A$ receptor antagonist bicuculline

methiodide, and the $GABA_A$ receptor agonist muscimol (all from Sigma, St Louis, MO, USA) to excite, disinhibit and inhibit the MnPN neurons, respectively.

The microdialysis procedure was carried out as described previously (Suntsova et al., 2007). The microdialysis probes (cuprophane semipermeable membrane length, 1 mm; outer diameter, 0.24 mm, molecular weight cut-off, 6000 Da; CMA/11, CMA Microdialysis Inc., North Chelmsford, MA, USA) were inserted into the implanted guide cannula 24 h before starting an experiment. The midline positioning of the probe at 15° angle from the vertical was chosen to minimize damage to the nucleus, which is narrow in mediolateral dimension. The tip of the probe was inside the very rostral part of the MnPN whereas the major part of the microdialysis membrane was in contact with a dorsal surface of the nucleus.

The probe was continuously perfused at a flow rate of 2.0 μl/min with filtered artificial cerebrospinal fluid (aCSF) containing (in mM): 145 NaCl, 2.7 KCl, 1.3 $MgSO_4$, 1.2 $CaCl_2$, and 2 Na_2HPO_4 (pH 7.2). All drugs were dissolved in this solution. Gastight Bee Stinger syringes were filled with perfusates at ambient temperature and mounted on Baby Bee Syringe Pumps connected to Bee Hive Pump controllers (Bioanalytical Systems, Inc, West Lafayette IN, USA). After delivery of substances, the perfusion solution was switched back to aCSF and the recording continued for another 45–90 min.

We estimate the effective spread of current and drugs as less than 0.25 mm and 0.75 mm, respectively (see for details Suntsova et al., 2007).

Experimental paradigms

Experiment 1

WAG/Rij ($n=12$) and Wistar ($n=12$) rats were divided into two subgroups. Experimental ($n=6$) and control ($n=6$) animals belonging to the first subgroup were allowed 2 h spontaneous sleep–waking behavior during the light phase of the light/dark cycle (ZT1–3). The equal number of animals from the second subgroup at the same circadian time was subjected to 2 h sleep deprivation by applying gentle arousing stimuli (tapping on the cage or slight cage movement) immediately after appearance of the first EEG correlates of NREM sleep. Animals were adapted to the sleep deprivation procedure for 5 days by exposing them to the same arousing stimuli for 5 min, 10 times per day. The polygraphic parameters were simultaneously monitored in 4 animals. In the first subgroup, one experimental and one control animal were chosen to be sacrificed immediately at the end of experiment if they showed more than 75% of sleep during both the first and the second hour of monitoring. In the second subgroup, a pair of experimental and control animals were killed right after the deprivation procedure.

Experiment 2

WAG/Rij ($n=12$) and ACI ($n=12$) rats were divided into 2 subgroups of six animals each. A first and a second subgroup were allowed spontaneous sleep–waking behavior during the light (ZT1–3) and dark (ZT 13–15) periods, respectively. Pairs of WAG/Rij and ACI rats that exhibited more than 75% of sleep during both hours of recording during the light period and less than 25% of sleep during the dark period were chosen to be sacrificed immediately after the end of the recording.

Experiment 3

Extracellular recordings were performed in eleven freely moving WAG/Rij rats during the light period (ZT 1–5) within the VLPO and MnPN. At the end of a recording session, under deep pentobarbital anesthesia (pentobarbital; 100 mg/kg, *i.p.*) microlesions were made at the tip of microwires (20 μA anodal direct current; 15–20 s) at the most ventral recorded site.

Experiment 4

EEG and EMG recordings were performed during the light period (ZT 1–10) in five freely moving Sprague–Dawley rats subjected to electrical stimulation of the MnPN. During the first experiment, the threshold for induction of absence-like seizures was detected by applying 10 s duration train stimulation (200 μs square pulses, 8–13 pulses/s) starting at 100 μA, increasing in 25 μA increments, delivered during waking with at least 10 min intervals. Stimulation was discontinued after appearance of the first SWDs. The stimulation protocol included three stimulations/day that were applied at this threshold intensity during waking, NREM and REM sleep with at least 1 h interval. Stimulation was discontinued after the first SWDs or 15 s if stimulation failed to induce SWDs. Since generalized tonic–clonic seizures were kindled, the effects of more prolonged stimulation, stimulation at higher intensities during seizure-resistant states, and high-frequency (100 pulses/s) stimulation were studied.

Experiment 5

The effects of chemical activation, disinhibition and inhibition of the MnPN neurons were studied in three rats.

Activation of MnPN neuronal populations without influence on passing fibers was achieved by microdialytic perfusion of excitatory amino acid L-glutamate at 1 mM and 10 mM concentrations. To disinhibit and inhibit MnPN neurons, the $GABA_A$ receptor antagonist, bicuculline, and $GABA_A$ receptor agonist, muscimol were perfused, respectively, both at 50 μM and 100 μM concentrations. Each day the effect of one drug at one concentration was tested. L-glutamate and bicuculline were perfused for 1 h during the dark phase of the light/dark cycle (ZT13–16), whereas muscimol was perfused for 15 min during the light phase (ZT3–6). Different circadian times were chosen to increase representation of wake–sleep transitions.

Histology and immunohistochemistry

Perfusion and tissue preparation

After a lethal dose of pentobarbital (100 mg/kg, i.*p.*), rats were injected with heparin (500 U, i.*p.*) and perfused transcardially with 30–50 ml of 0.1 M phosphate buffer (pH 7.2) for 5 min followed by 300 ml of 4% paraformaldehyde (PFA) in phosphate buffer containing 15% saturated picric acid solution. The brains were removed, postfixed in the same PFA solution for 20 min and equilibrated in 10, 20 and 30% sucrose in PBS at 4 °C until they sank. Coronal sections were cut through the preoptic area at 30-μm thickness on a freezing microtome and were stored in cryoprotectant at −20 °C until staining.

Immunohistochemistry

Free-floating sections were sequentially immunostained for c-Fos protein and for glutamic acid decarboxylase (GAD) as described previously (Gvilia et al., 2006). Briefly, for c-Fos staining, a rabbit polyclonal anti-c-Fos antiserum (AB5; 1:15,000; Oncogene Sciences, Cambridge, MA) and a biotinylated goat anti-rabbit IgG (BA-100; 1:800; Vector Laboratories, Burlingame, CA) were used as primary and secondary antibodies, respectively. Signal amplification was achieved using the avidin–biotin complex (ABC, Vector Elite kit; 1:200;Vector Laboratories, Burlingame, CA). Nickel- 3, 3′-diaminobenzidine (DAB, Sigma, St. Louis, MO) was used as the chromagen. Black nuclear staining indicated c-Fos-immunoreactivity (IR). Omission of the c-Fos primary antiserum resulted in the absence of staining. Normal rabbit IgG was used instead of the primary antibody as a negative control. For GAD staining, a mouse anti-GAD67 monoclonal primary antibody (MAB5406; 1:300; Chemicon, Temecula, CA) and a biotinylated horse anti-mouse secondary antibody (BA-2001, 1:300; Vector Laboratories, Burlingame, CA) were used followed by reaction with ABC (1:150, Vector Laboratories, Burlingame, CA). GAD-immunoreactivity was visualized using DAB which produced brown reaction product in the cytoplasm. Omission of the GAD primary antiserum resulted in the

absence of staining. Twelve sets of sections from experimental ($n=6$) and control ($n=6$) animals with equally represented predominantly asleep and predominantly awake rats were processed simultaneously.

Histology

Serial coronal sections (40 μm) were stained for Nissl (cresyl violet) to verify the position of the microwire tracks. In several cases sections were immunostained for GAD as described previously.

Reconstructions of tracts of microwires, stimulation electrodes, and microdialysis probes were made with the aid of Neurolucida imaging system (MicroBrightField, Colchester, VT) guided by the rat brain atlases of Swanson (1998) for the MnPN and Paxinos and Watson (1998) for the VLPO. According to reconstructions, microwires were correctly positioned in the MnPN in six rats and in the VLPO in five rats (Fig. 1B). From these animals, 95 and 32 cells recorded within the MnPN and VLPO, respectively, with signal-to-noise ratio >3 (Fig. 1A), were examined for their sleep–wake discharge patterns. Stimulating electrodes and microdialysis probes were correctly positioned within the MnPN in 5 and 3 rats, respectively (Fig. 1C).

Data analysis

Sleep–wake analysis and detection of SWDs

Sleep–wake states of the rats during 2 h recordings in Experiment 1 and Experiment 2 were roughly determined on-line by the experimenter and then off-line by the trained scorer blind to the experimental condition and group identity of the animal. In the latter case scoring was performed on the basis of the predominant state within each 10 s epoch. Wakefulness (W), NREM and REM sleep were identified on the basis of EEG and EMG parameters using standard criteria (Timo-Iaria et al., 1970). SWDs were detected by visual inspection based on the standard criteria for type I SWDs (Van Luijtelaar and Coenen, 1986).

Cell counts

GAD-immunoreactive (GAD^+), c-Fos-immunoreactive ($c\text{-}Fos^+$) and double-labeled for c-Fos and GAD ($c\text{-}Fos^+/GAD^+$) neurons were identified and quantified using Neurolucida computer-aided plotting system (MicroBrightField, Williston, VT) by an observer blind

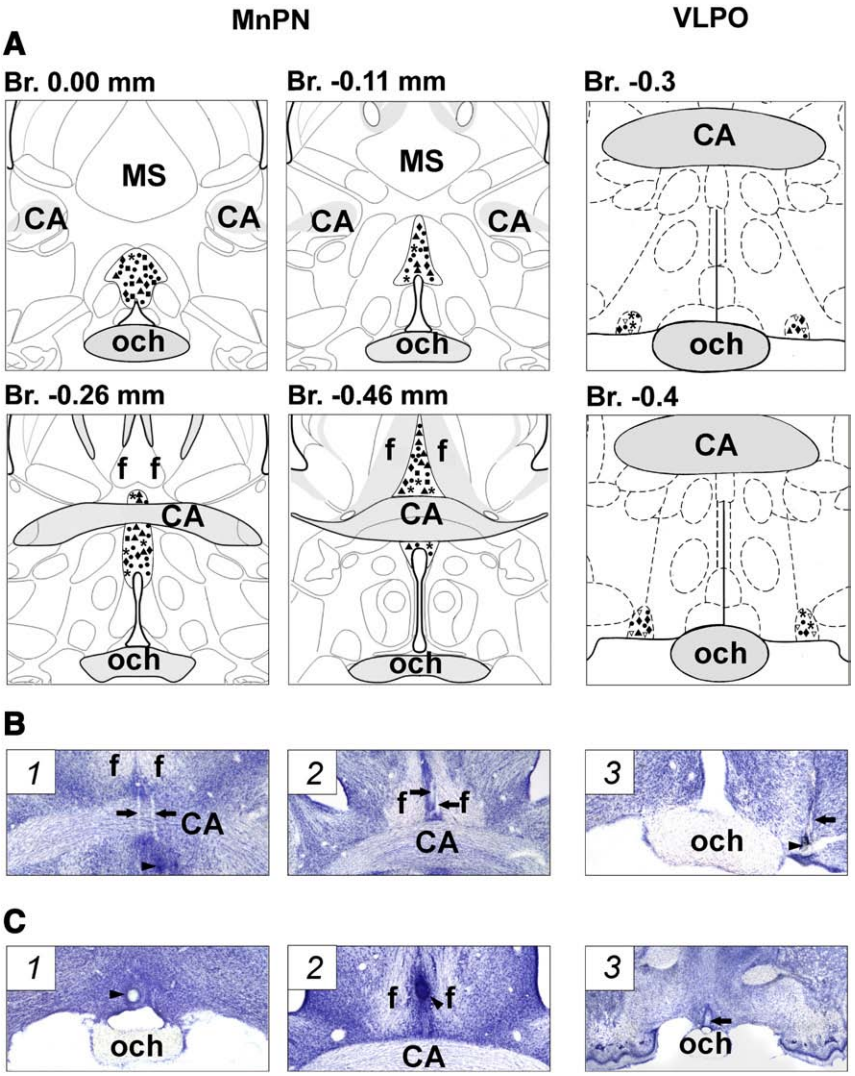

Fig. 1. Anatomical localization of recorded neurons, stimulating electrodes, and microdialysis probes. (A) schematic drawings showing locations of recorded MnPN and VLPO neurons with different sleep–wake discharge profiles: NREM/REM sleep-related (black up triangles), NREM sleep-related (squares), REM sleep-related (asterisks), W/REM sleep-related (diamonds), W-related (down unfilled triangles), and state-indifferent (circles) neurons within the MnPN and VLPO. For better visualization the locations of VLPO neurons are plotted on the maps bilaterally. (B) photomicrographs of Nissl-stained coronal sections showing the locations of microwire tracks (arrows) within rostral MnPN (1), caudal MnPN (2) and VLPO (3). Arrowheads indicate electrolytic lesions at the sites of the most ventral recordings. (C) photomicrographs of Nissl-stained sections showing the locations of stimulating electrodes and microdialysis probes. Arrowheads indicate the sites of electrolytic lesions within the rostral (1) and caudal (2) MnPN. Arrow shows the track of the tip of microdialysis probe within the rostral MnPN (3). CA, commissure anterior; MS, medial septum: och, optic chiasm; f, fornix.

to the experimental condition and group identity of the animals. Section outlines were drawn under 20× magnification and the cells were mapped in the outlines under 400× magnification. Cell counts were done in three sections within constant rectangular grids corresponding to five areas of interest. (1) The rostral MnPN grid was a 600×600 μm square, centered on the apex of the third ventricle rostral to the decussation of the anterior commissure and to bregma (anterior, 0.1 mm) (Gong et al., 2000). (2) The caudal MnPN grid was placed immediately dorsal to the third ventricle at the level of the decussation of the anterior commissure, extending 150 μm laterally and 600 μm dorsally (Gong et al., 2000). The VLPO counting grids were placed bilaterally at three sections at AP level from −0.3 to −0.7 mm relative to bregma and subdivided into core and extended sections (Lu et al., 2002). (3) The VLPO core box was 300 μm wide by 300 μm high, placed along the base of the brain, with its far border 400 μm lateral to the lateral edge of the optic chiasm. (4) The medial extended VLPO box was medial to the VLPO core, 400 μm wide by 300 μm high. (5) The dorsal extended VLPO box was 200 μm wide by 300 μm high, positioned above the VLPO core and medial extended VLPO boxes and centered over their border. Cell counts within each grid were made in three sections and averaged to yield a single value for each rat. For the VLPO, cell counts were made bilaterally.

Neuronal discharge

The mean firing rates of MnPN and VLPO neurons were calculated off-line for ten 15–60 s artifact-free periods of W, NREM, and REM sleep using Spike2 software package (Cambridge Electronic Design, London, UK).

In order to classify the recorded cells into groups with different sleep–wake discharge profiles, multivariate (*k*-means cluster) analysis was performed as described previously (Suntsova et al., 2002). To reach appropriate classification (in terms of fullness of representation of sleep–wake discharge patterns and within/between-cluster variability) the number of clusters (*k*) was gradually increased until further increase in *k* did not result in appearance of clusters with new discharge profiles. Cluster analysis was followed by analysis of significance changes in the mean firing rates within each cluster and evaluation of state-relatedness for each member of the cluster.

To compare neuronal discharge in WAG/Rij and non-epileptic rats, our previous data on firing rates of individual VLPO and MnPN cells across sleep–wake states in non-epileptic Sprague–Dawley rats were used (Szymusiak et al., 1998; Suntsova et al., 2002).

Statistical analysis

All results are reported as mean ± SEM. Statistical comparisons were performed by Student's *T*-test, one- and two-way analysis of variance (ANOVA). Significant main effects were followed by Tukey's HSD *post hoc* test. Significant interactions were analyzed by simple main effects (one-way ANOVA).

Results

Experiments 1 and 2: effects of sleep–wake state and strain on MnPN and VLPO c-Fos expression in WAG/Rij and non-epileptic control rats

Sleep–wake parameters and spike-wave discharges

Table 1 shows the percentages of NREM sleep, REM sleep and W during 2 h prior to sacrifice in Experiments 1 and 2. The percent of total sleep did not differ significantly in WAG/Rij and Wistar rats in matched experimental conditions including spontaneous sleep–wake behavior or sleep deprivation during the light phase of the light/dark cycle (Experiment 1) and in WAG/Rij and ACI rats that were allowed spontaneous sleep–waking behavior during the light or dark phases (Experiment 2). Each undisturbed experimental and control rat spent more than 75% of the time in sleep during the light period and accumulated less than 25% of sleep during the dark period (spontaneously predominantly asleep and predominantly awake animals are referred to as "sleeping" and "awake" later in the text). Each sleep-deprived rat was asleep less than 7% of the time, and exhibited only NREM sleep (Table 1). The only statistically significant difference in the percentages of sleep–wake states between experimental and control animals was found for percent of REM sleep during the light phase of the light/dark cycle both in Experiment 1 and Experiment 2 ($p<0.05$, Student's *T*-test).

All WAG/Rij rats exhibited SWDs with characteristics like those described in numerous previous studies (rev. in Coenen and van Luijtelaar (2003)). In both experiments the incidence of SWDs was the lowest early in the light phase when animals were predominantly asleep (Table 1). During sleep deprivation treatments in the light phase (Experiment 1) and during spontaneous predominantly awake behavior in the early dark phase (Experiment 2) the number of SWDs was significantly higher ($p<0.001$, Student's *T*-test) (Table 1).

C-Fos immunoreactivity

Representative examples of the distribution of single labeled Fos^+ neurons and Fos^+ GABAergic cells within the MnPN and VLPO in sleeping and spontaneously awake or sleep-deprived WAG/Rij and control rats are shown in Figs. 2 and 3, respectively. The mean numbers of Fos^+ neurons, Fos^+/GAD^+ cells and mean percentages of GAD^+ neurons expressing c-Fos within the MnPN and VLPO across all groups of animals are shown in Fig. 4.

Median preoptic nucleus

A two-way ANOVA (2×2 factorial design with strain and behavioral state as between-subjects factors) revealed statistically significant strain×behavioral state interactions within the rostral MnPN in Experiments 1 and 2 and within the caudal MnPN in Experiment 2 for each parameter studied, including the mean number of c-Fos^+ cells, c-Fos^+/GAD^+ neurons and % GAD^+ cells expressing c-

Table 1
Sleep–wake cycle parameters and spike-wave discharges in Experiment 1 and Experiment 2.

Sleep–wake states	Experiment 1				Experiment 2			
	Spontaneous behavior (light phase)		Sleep deprivation (light phase)		Spontaneous behavior (light phase)		Spontaneous behavior (dark phase)	
	WAG/Rij ($n=6$)	Wistar ($n=6$)	WAG/Rij ($n=6$)	Wistar ($n=6$)	WAG/Rij ($n=6$)	ACI ($n=6$)	WAG/Rij ($n=6$)	ACI ($n=6$)
Wakefulness (%)	17.6 ± 0.9	18.7 ± 1.2	94.5 ± 0.7	95.9 ± 0.8	18.7 ± 1.0	19.7 ± 1.5	80.4 ± 1.5	78.6 ± 1.5
Non-REM sleep (%)	72.4 ± 1.3	70.4 ± 1.2	5.5 ± 0.7	4.1 ± 0.8	70.3 ± 1.5	65.8 ± 1.5	16.5 ± 1.6	17.3 ± 0.8
REM sleep (%)	10.0 ± 0.8	12.9 ± 0.6*	0	0	11.0 ± 1.1	14.5 ± 1.0*	3.1 ± 0.4	4.1 ± 0.7
Number of SWDs	10.7 ± 0.9***	0	21.3 ± 1.5	0	11.2 ± 1.2***	0	20.0 ± 1.8	0

Shown is the percentage of time spent in wakefulness, REM sleep, and non-REM sleep for WAG/Rij and control rats that were allowed spontaneous sleep–waking behavior ($n=6$) or were subjected to sleep deprivation ($n=6$) during the light phase of the light–dark cycle (Experiment 1) or were allowed spontaneous behavior during the light ($n=6$) and dark ($n=6$) phases (Experiment 2). Percentages of sleep–waking stages were calculated for a 2 h period prior to sacrifice. No significant strain differences in percentages of wakefulness and NREM sleep for each experimental condition were found. Undisturbed WAG/Rij rats, compared to both Wistar and ACI rats exhibited lower percent REM sleep during the light phase of the light/dark cycle ($p<0.05$, Student's *T*-test). The incidence of the SWDs in WAG/Rij rats in predominantly asleep condition during the light phase was lower than during sleep deprivation and predominantly awake condition in the dark phase ($p<0.001$, Student's *T*-test).

* $p<0.05$.
*** $p<0.001$.

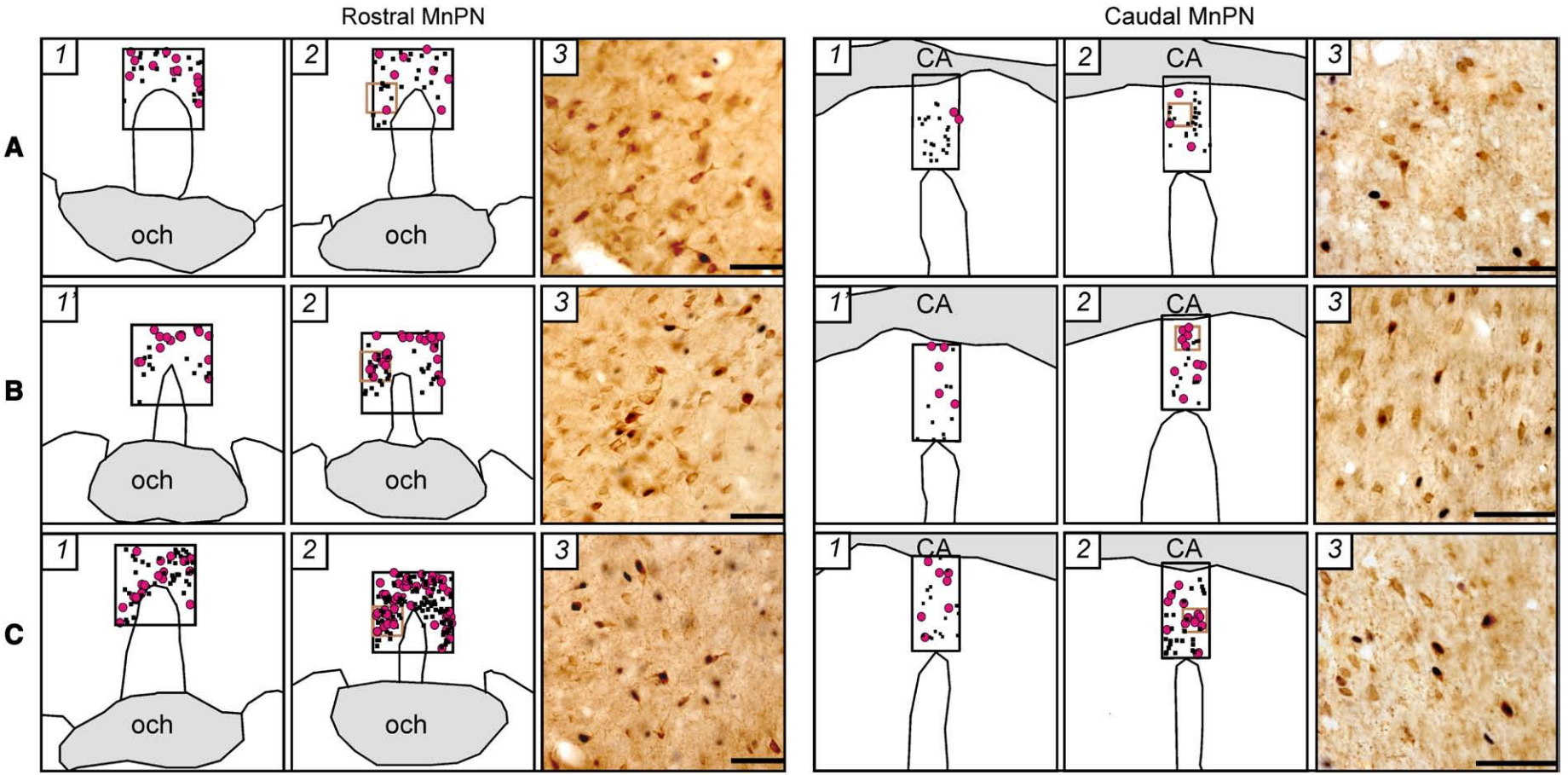

Fig. 2. A–C, Representative examples of distribution of c-Fos^{+} (black dots) and c-Fos^{+}/GAD^{+} (pink circles) neurons within the rostral and caudal MnPN in line drawings from WAG/Rij (A), Wistar (B) and ACI (C) rats that during 2 h prior to sacrifice were spontaneously predominantly awake (1), sleep-deprived (1') or predominantly asleep (2). Photomicrographs (3) correspond to the areas marked as brown squares in 2. The c-Fos protein is stained black and confined to the nucleus. The GAD-immunoreactive neurons are stained brown, and the staining is evident throughout the soma and the proximal dendrites. CA, commissure anterior; och, optic chiasm. Horizontal bar, 50 μm.

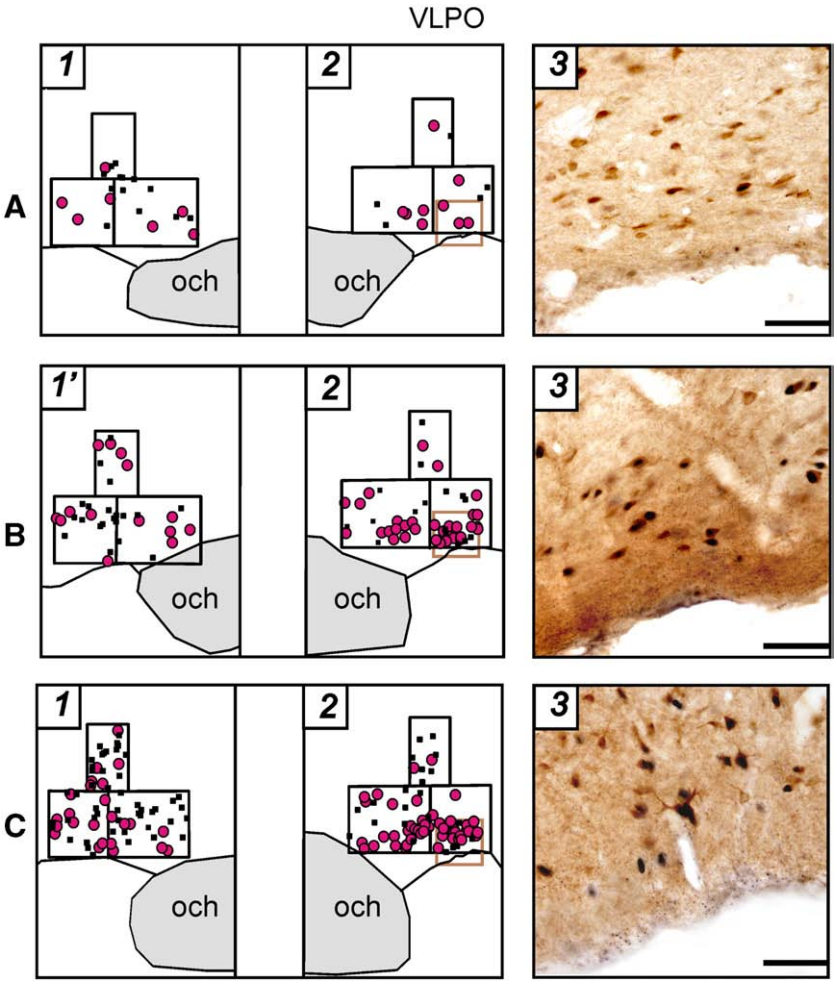

Fig. 3. A–C, Representative examples of distribution of c-Fos$^+$ and c-Fos$^+$/GAD$^+$ neurons within the VLPO cluster, dorsal and medial extended VLPO in line drawings from WAG/Rij (A), Wistar (B) and ACI (C) rats that during 2 h prior to sacrifice were predominantly spontaneously awake (1) or sleep-deprived (1) and predominantly asleep (2). Photomicrographs (3) correspond to the areas marked as brown squares in *2*. Och, optic chiasm. Horizontal bar, 50 μm.

Fos (Table 2). Within the caudal MnPN in Experiment 1 neither significant main effects of factors nor interaction between the factors were found for all the parameters (Table 2). Analyses for simple main effects (one-way ANOVAs), required in case of the presence of significant interaction and defensible in case of the absence of significant main effects and interaction (Tybout and Sternthal, 2001), were then applied to the data.

The effect of the behavioral state on total c-Fos immunoreactivity and c-Fos activation of GABAergic neurons depended on the rat strain. In WAG/Rij rats no significant differences were found between sleeping and sleep-deprived animals (Experiment 1), or between sleeping and spontaneously awake rats (Experiment 2) in any parameter studied within both rostral and caudal MnPN sites (Figs. 4A, B). Non-epileptic control rats exhibited sleep-associated increases in total c-Fos expression and/or in c-Fos activation of GABAergic neurons. Within the rostral MnPN (Fig. 4A), both Wistar and ACI rats exhibited higher numbers of c-Fos$^+$ cells ($F_{(1,\ 10)}=12.6$ and $F_{(1,\ 10)}=12.1$, respectively, $p<0.01$), c-Fos$^+$/GAD$^+$ cells ($F_{(1,\ 10)}=11.1$, $p<0.01$ and $F_{(1,\ 10)}=6.9$, $p<0.05$, respectively) and % GAD$^+$ cells expressing c-Fos ($F_{(1,\ 10)}=6.8$ and $F_{(1,\ 10)}=8.6$, respectively, $p<0.05$) in sleeping compared to sleep-deprived/spontaneously awake conditions (Fig. 4A). Within the caudal MnPN, in Wistar rats (Experiment 1) the number and % GABAergic cells expressing c-Fos were significantly higher ($F_{(1,\ 10)}=7.2$, $p<0.05$ and $F_{(1,\ 10)}=5.8$, $p<0.05$, respectively) in sleeping animals compared to sleep-deprived (Fig. 4B). The difference in the total number of c-Fos$^+$ cells approached statistical significance ($F_{(1,\ 10)}=4.2$, $p=0.06$). In ACI rats (Experiment 2) total c-Fos expression and c-Fos immunoreactivity in subpopulation of GABAergic cells tended to be higher in sleeping condition ($F_{(1,\ 10)}=3.9$, $p=0.08$ and $F_{(1,\ 10)}=3.8$, $p=0.08$, respectively) (Fig. 4B).

Strain differences in total c-Fos immunoreactivity and/or in c-Fos activation of GABAergic neurons were found in sleeping but not in sleep-deprived/spontaneously awake rats. Within the rostral MnPN, sleeping WAG/Rij rats, compared to sleeping Wistar and ACI rats exhibited lower total c-Fos immunoreactivity ($F_{(1,\ 10)}=14.3$, $p<0.01$ and $F_{(1,\ 10)}=156.3$, $p<0.001$, respectively), the number ($F_{(1,\ 10)}=67.8$ and $F_{(1,\ 10)}=29.3$, respectively, $p<0.001$) and percentage ($F_{(1,\ 10)}=52.4$ and $F_{(1,\ 10)}=25.5$, respectively, $p<0.001$) of GABAergic cells expressing c-Fos (Fig. 4A). Within the caudal MnPN, in Experiment 1 the number of c-Fos$^+$ GABAergic cells tended to be lower $F_{(1,\ 10)}=3.8$, $p=0.08$) and % GABAergic neurons expressing c-Fos was significantly lower $F_{(1,\ 10)}=5.7$, $p<0.05$) in sleeping WAG/Rij compared to sleeping Wistar rats (Fig. 4B). In Experiment 2 sleeping WAG/Rij, compared to sleeping ACI rats exhibited significantly lower total c-Fos immunoreactivity ($F_{(1,\ 10)}=11.8$, $p<0.01$), the number and % of GABAergic cells with c-Fos-immunoreactive nuclei ($F_{(1,\ 10)}=23.0$, $p<0.001$ and $F_{(1,\ 10)}=34.8$, $p<0.001$, respectively) (Fig. 4B).

Ventrolateral preoptic area

In both experiments the pattern of inter-state and inter-strain differences in c-Fos expression within the VLPO cluster was similar to that within the medial, but not dorsal extended VLPO.

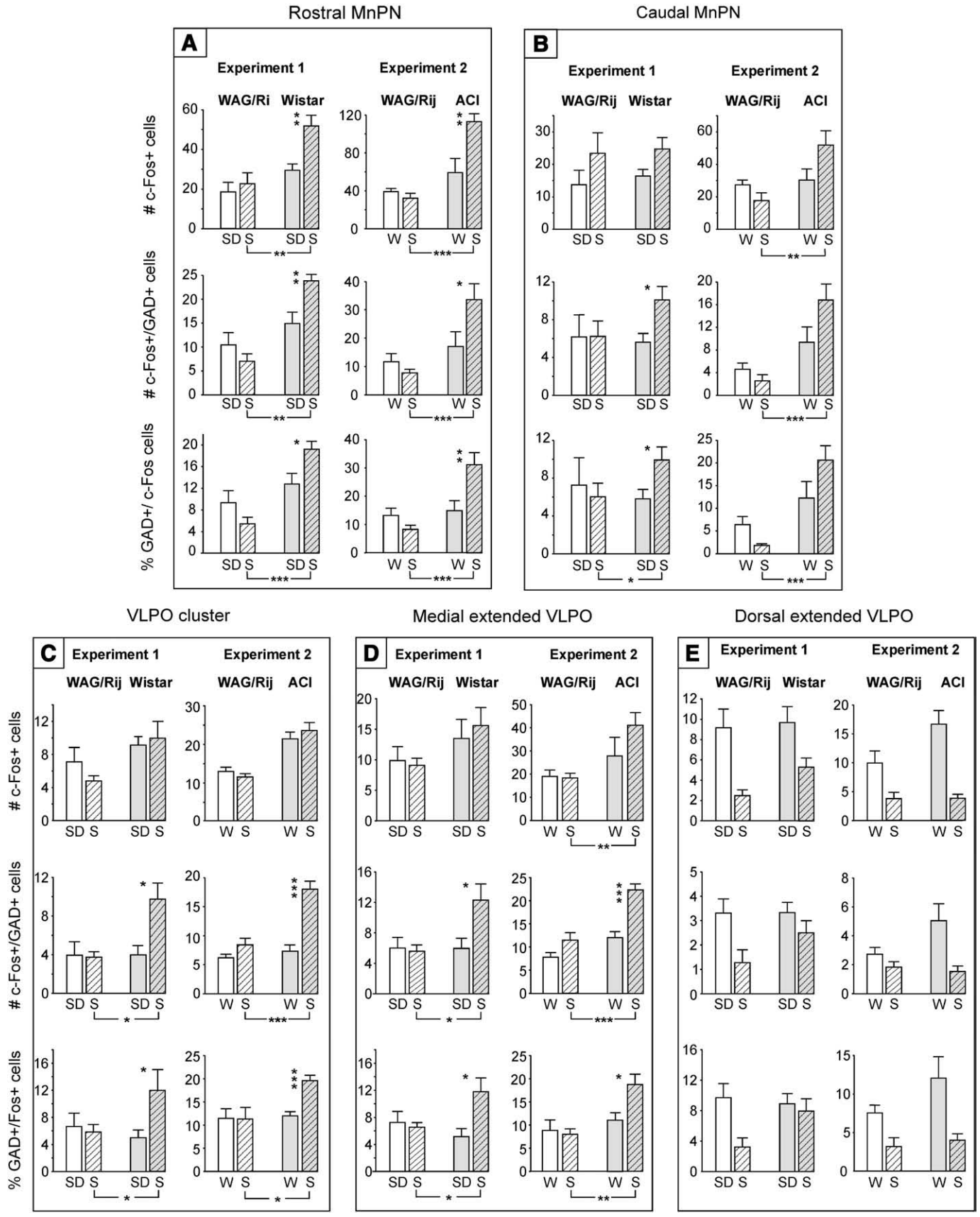

Fig. 4. The mean numbers of c-Fos$^+$ neurons, c-Fos$^+$/GAD$^+$ cells and mean percentages of GAD$^+$ neurons expressing c-Fos within the MnPN and VLPO in WAG/Rij and control rats in Experiment 1 and Experiment 2. White bars, WAG/Rij rats; grey bars, control rats. SD, sleep-deprived animals, W, spontaneously predominantly awake animals, S, predominantly asleep animals. Note that epileptic WAG/Rij rats do not exhibit sleep-related increase in total c-Fos immunoreactivity and in c-Fos activation of GABAergic neurons. *$p<0.05$; **$p<0.01$; ***$p<0.001$, one-way ANOVA. See Table 2 for significance of main effect of factor Strain on total number of c-Fos$^+$ cells within the VLPO cluster and main effect of factor Behavioral State on all parameters within the dorsal extended VLPO.

Table 2
Two-way ANOVA results: main effects and interaction of factors strain (S) and behavioral state (BS).

Structure		Experiment 1									Experiment 2								
		# c-Fos$^+$ cells			# c-Fos$^+$/GAD$^+$ cells			% GAD$^+$ cells expressing c-Fos			# c-Fos$^+$ cells			# c-Fos$^+$/GAD$^+$ cells			% GAD$^+$ cells expressing c-Fos		
		SxBS	S	BS	SxBS	S	BS	SxBS	S	BS	SxBS	S	BS	SxBS	S	BS	SxBS	S	BS
Rostral MnPN	$F_{(1, 20)}$	4.8[a]			9.4[b]			8.5[b]			13.2[b]			9.0[b]			11.4[b]		
Caudal MnPN	$F_{(1, 20)}$	NS	NS	NS	NS	NS	NS	NS	NS	NS	6.5[a]			5.2[a]			6.3[a]		
VLPO cluster	$F_{(1, 20)}$	NS	5.8[a]	NS	4.4[a]			4.5[a]			NS	46.0[c]	NS	15.0[c]			4.7[a]		
Medial extended VLPO	$F_{(1, 20)}$	NS	NS	NS	4.7[a]			4.5[a]			NS	NS	NS	6.0[a]			5.4[a]		
Dorsal extended VLPO	$F_{(1, 20)}$	NS	NS	17.2[c]	NS	NS	8.0[a]	NS	NS	5.5[a]	NS	NS	30.6[c]	NS	NS	9.4[b]	NS	NS	13.2[b]

The main effects of factors that were not interpreted due to the presence of significant interaction are not shown.
[a] $p<0.05$.
[b] $p<0.01$.
[c] $p<0.001$.

Within the VLPO cluster and medial extended VLPO in both experiments factor behavioral state did not affect the total c-Fos expression, and no significant behavioral state × strain interactions were found (two-way ANOVA, Table 2). Within the VLPO cluster, the main effect of factor strain was statistically significant (Table 2). The number of c-Fos-immunoreactive cells was lower in WAG/Rij rats compared to Wistar and ACI rats ($F_{(1, 20)}=5.8$, $p<0.05$ and $F_{(1, 20)}=46.0$, $p<0.001$, respectively) (Fig. 4C). Within the medial extended VLPO the main effect of factor strain was insignificant.

Two-way ANOVA performed for the number and % GABAergic cells expressing c-Fos showed the presence of a significant interaction between the factors strain and behavioral state within both the VLPO cluster and medial extended VLPO in Experiments 1 and 2 (Table 2). As in the MnPN, the behavioral state effect on these parameters was strain-depended. In WAG/Rij rats the inter-state differences in c-Fos activation of GABAergic neurons were insignificant (Figs. 4C, D). In control animals, the number and % GAD$^+$ neurons expressing c-Fos was higher in sleeping compared to sleep-deprived Wistar rats (VLPO cluster, $F_{(1, 10)}=5.7$, and $F_{(1, 10)}=5.5$, respectively; medial extended VLPO, $F_{(1, 10)}=5.0$ and $F_{(1, 10)}=6.6$, respectively, $p<0.05$) and in sleeping compared to spontaneously awake ACI rats (VLPO cluster, $F_{(1, 10)}=35.8$ and $F_{(1, 10)}=32.3$, respectively, $p<0.001$; medial extended VLPO, $F_{(1, 10)}=28.3$, $p<0.001$ and $F_{(1, 10)}=7.7$, $p<0.05$, respectively) (Figs. 4C, D).

Strain differences in c-Fos activation of GABAergic cells were statistically significant only in sleeping condition. The number and % GABAergic neurons expressing c-Fos were significantly lower in WAG/Rij compared to Wistar rats in Experiment 1 (VLPO cluster, $F_{(1, 10)}=7.6$ and $F_{(1, 10)}=5.1$, respectively, $p<0.05$; medial extended VLPO, $F_{(1, 10)}=7.3$ and $F_{(1, 10)}=5.7$, respectively, $p<0.05$) and compared to ACI rats in Experiment 2 (VLPO cluster, $F_{(1, 10)}=28.2$, $p<0.001$ and $F_{(1, 10)}=8.5$, $p<0.05$, respectively; medial extended VLPO, $F_{(1, 10)}=25.4$, $p<0.001$ and $F_{(1, 10)}=18.3$, $p<0.01$, respectively) (Figs. 4C, D).

Within the dorsal extended VLPO, two-way ANOVA revealed significant main effect of factor behavioral state, insignificant main effect of factor strain and insignificant strain × behavioral state interactions in both experiments for all the parameters studied (Table 2). Total c-Fos expression and c-Fos activation of GABAergic neurons was lower in sleeping rats compared to sleep-deprived (Fig. 4E).

Experiment 3: sleep–wake discharge patterns of MnPN and VLPO neurons

The overall statistical characteristics of discharge frequency of 95 MnPN neurons and 32 VLPO cells recorded in WAG/Rij rats during W, NREM and REM sleep are shown in Table 3.

The results of *k*-means cluster analyses applied for classification of sleep–wake discharge profiles of MnPN and VLPO neurons are shown in Figs. 5A and 6A, respectively. The full representation of sleep–wake discharge patterns was achieved when the number of clusters for the MnPN and VLPO neurons was specified as ten and six, respectively. In some clusters, neurons exhibited the same trend of changes in the mean firing rates but differed in the level of firing. Within each cluster of state-related cells the changes in the mean firing rate across sleep–wake cycle were statistically significant (Figs. 5A and 6A). Recorded cells were subdivided into sleep-related, W/REM sleep-related, W-related and state-indifferent neuronal groups. According to the specificity of discharge changes during sleep, sleep-related neurons were identified as NREM/REM-, NREM-, or REM sleep-related. NREM/REM sleep-related cells increased their firing rates during both phases of sleep compared to waking. Discharge of NREM and REM sleep-related cells during NREM and REM sleep, respectively, was significantly higher compared to the rest sleep–wake states.

Sleep-related neurons

In WAG/Rij rats 45.3% MnPN cells and 18.7% VLPO neurons discharged at higher rates during one or both phases of sleep compared to W. The percentages of sleep-related neurons in genetic absence epilepsy rats were lower than in non-epileptic Sprague–Dawley rats. In our previous studies in non-epileptic rats 76.4% MnPN cells

Table 3
Statistical characteristics of discharge rate (spikes/s) of MnPN neurons ($n=95$) and VLPO neurons ($n=32$) during different stages of the sleep–waking cycle.

Sleep–wake state	Mean ± SEM		Median		Range		Coefficient of variation (%)	
	MnPN	VLPO	MnPN	VLPO	MnPN	VLPO	MnPN	VLPO
Wakefulness	2.6 ± 0.3	5.6 ± 0.9	1.6	3.2	0.05–16.6	0.2–17.1	125.0	92.9
NREM sleep	2.8 ± 0.2	4.4 ± 1.3	2.3	2.5	0.1–8.5	0.01–32.5	71.7	165.9
REM sleep	4.4 ± 0.4*** a, b	7.2 ± 1.8* b	2.9	2.7	0.1–15.8	0.3–41.2	98.4	138.3
Main effect of sleep–wake state	$F_{(2, 188)}=25.8$ $p<0.001$	$F_{(2, 62)}=3.6$, $p<0.05$						

One-way repeated measures ANOVA revealed significant main effect of sleep–wake state on MnPN and VLPO neuronal discharge. Within the MnPN, significant pair-wise differences (Tukey's *post hoc* test) in the group mean firing rate were found between REM sleep and wakefulness (a) and REM sleep and NREM sleep (b) with an increased discharge during REM sleep. Within the VLPO, the mean firing rate in REM sleep was significantly higher only compared to NREM sleep (b).
* $p<0.05$.
*** $p<0.001$, Tukey's *post hoc* test.

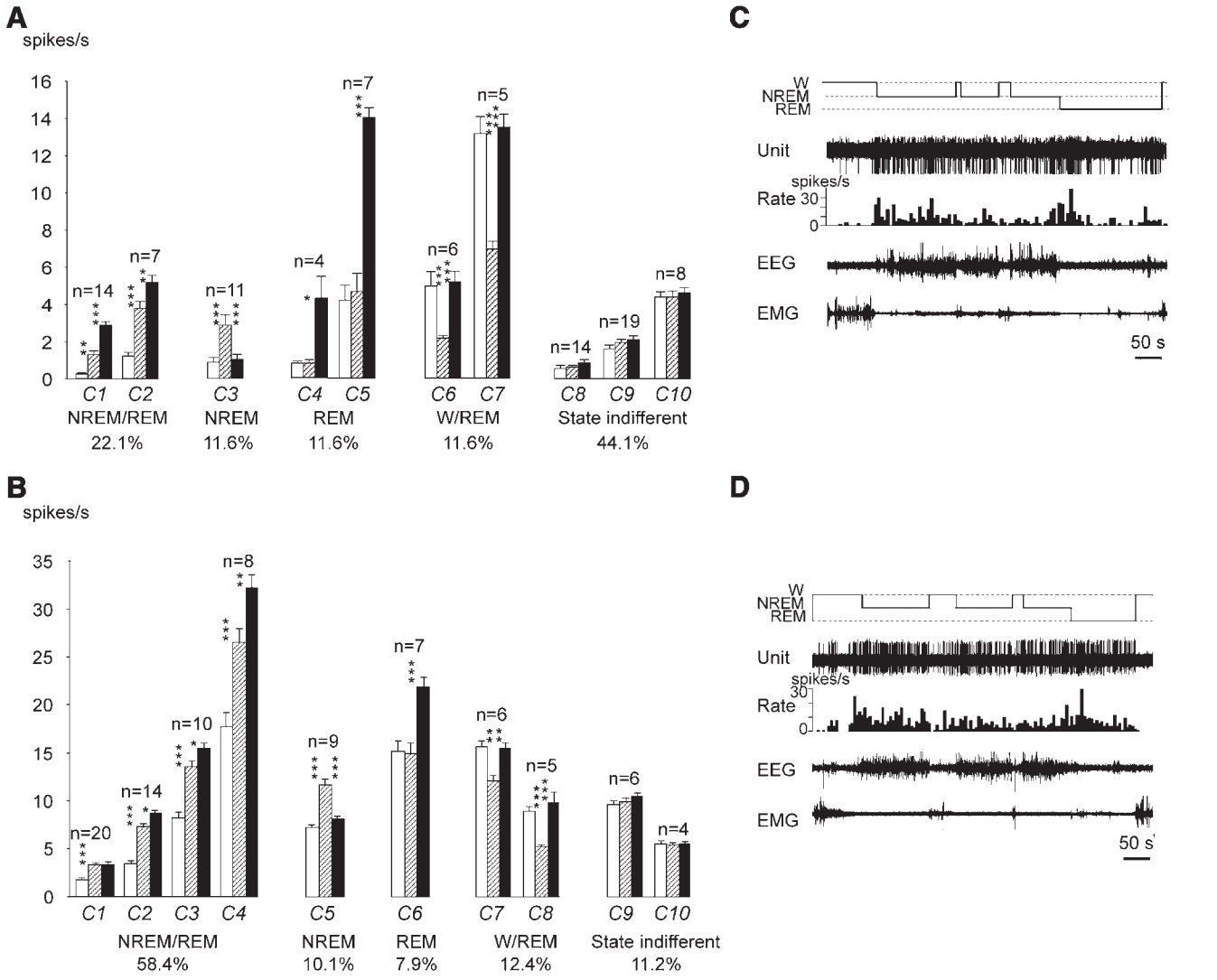

Fig. 5. A, Sleep–wake discharge profiles of MnPN neurons in WAG/Rij rats. Based on the results of the cluster-analysis, recorded cells were subdivided into 10 clusters (*C1–10*) and then classified into 5 groups with different sleep–wake discharge profiles: NREM/REM sleep-related (*C1–2*), NREM sleep-related (*C3*), REM-sleep-related (*C4–5*), W/REM sleep-related (*C6–7*), and state-indifferent cells (*C8–10*). Within each cluster of state-related cells the mean firing rate in the course of the sleep–waking cycle changed significantly (*C1*, $F_{(2,\ 12)}=79.1$; *C2*, $F_{(2,\ 26)}=62.6$; *C3*, $F_{(2,\ 20)}=33.5$; *C4*, $F_{(2,\ 6)}=10.6$; *C5*, $F_{(2,\ 12)}=107.8$; *C6*, $F_{(2,\ 10)}=17.3$; C7, $F_{(2,\ 8)}=52.3$; $p<0.05$ for *C4*, $p<0.001$ for the rest of the clusters, one-way repeated measures ANOVA). White bars, wakefulness; dashed bars, NREM sleep; black bars, REM sleep. B, sleep–wake discharge profiles of MnPN neurons in non-epileptic Sprague–Dawley rats (data are taken from Suntsova et al., 2002). Note that all types of sleep–wake discharge patterns previously found in non-epileptic rats were represented in WAG/Rij rats. However, WAG/Rij rats exhibited lower % NREM/REM sleep-related cells, which lacked clusters with >10 pulses/s sleep firing rate, and higher % state-indifferent neurons. C, D, discharge patterns of individual NREM/REM sleep-related MnPN neurons recorded across sleep–wake states in WAG/Rij (C) and Sprague–Dawley (D, the figure is taken from Suntsova et al., 2002*)* rats. Note that the cells fire at comparable rates and similarly change their discharge during sleep gradually decreasing firing rates during individual NREM sleep episodes and their sequences as well as during REM sleep. *$p<0.05$; ⁂$p<0.01$; ⁂$p<0.001$, Tukey's *post-hoc* test

(Suntsova et al., 2002) and 56.1% VLPO cells (Szymusiak et al., 1998) were sleep-related.

Within the MnPN, the percentage of NREM/REM sleep-related neurons in WAG/Rij rats (22.1%) was lower ($p<0.001$, Student's *T*-test) than in non-epileptic rats (58.4%), whereas the differences in percentages of the remaining types of sleep-related cells were not significant (Figs. 5A, B).

A two-way repeated measures ANOVA with sleep–wake state as a within-subjects factor with 3 levels (W, NREM and REM sleep) and strain as a between-subjects factor was used to compare the mean firing rates of MnPN sleep-related cells in WAG/Rij and non-epileptic Sprague–Dawley rats. Factor strain significantly affected the mean firing rate of NREM/REM sleep-related ($F_{(1,\ 71)}=12.8$, $p<0.001$), NREM sleep-related $F_{(1,\ 17)}=203.6$, $p<0.001$), and REM sleep-related ($F_{(1,\ 16)}=48.2$, $p<0.001$) cells. All types of sleep-related neurons discharged at lower rates in WAG/Rij rats across all examined sleep–wake states (Figs. 5A, B).

Within the VLPO, only two NREM/REM sleep-related and four REM sleep-related neurons were recorded in WAG/Rij rats (Fig. 6A). Given the low number of NREM/REM sleep-related cells in WAG/Rij rats, absence of NREM sleep-related neurons in WAG/Rij and REM sleep-related cells in non-epileptic Sprague–Dawley rats, the comparison of strain differences in firing rates of sleep-related VLPO cells was not performed.

W/REM sleep-related neurons and W-related neurons

The firing rate of W/REM sleep-related cells during both W and REM sleep was significantly higher compared to NREM sleep. Discharge of W-related neurons during waking was significantly elevated compared to both phases of sleep.

Within the MnPN, the percentage of W/REM sleep-related neurons in WAG/Rij rats (11.6%) was almost the same as in non-epileptic rats (12.4%) (Figs. 5A, B). A two-way ANOVA did not reveal significant differences in the mean firing rates of W/REM sleep-

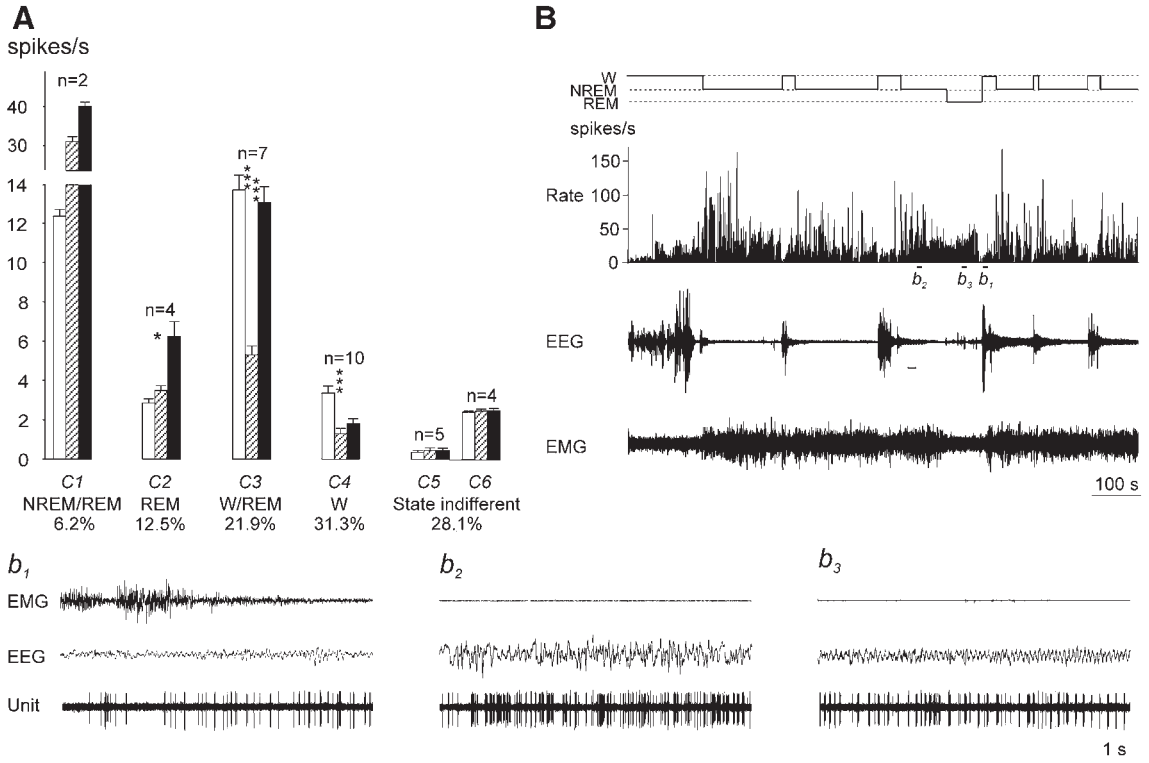

Fig. 6. (A) Sleep–wake discharge profiles of VLPO neurons in WAG/Rij rats. Based on the results of the cluster-analysis, recorded cells were subdivided into 6 clusters (*C1–6*) and then classified into 5 groups with different sleep–wake discharge profiles: NREM/REM sleep-related (*C1*), NREM, REM-sleep-related (*C2*), W/REM sleep-related (*C3*), wake-related (*C4*), and state-indifferent cells (*C5–6*). Within the clusters of state-related cells the mean firing rate in the course of the sleep–waking cycle changed significantly (*C2*, $F_{(2,\ 6)} = 11.7$, $p<0.01$, *C3*, $F_{(2,\ 12)} = 80.6$, $p<0.001$; *C4*, $F_{(2,\ 18)} = 33.3$, $p<0.001$, one-way repeated measures ANOVA; significance of changes within the *C1* was not estimated due to the low number of the members of this cluster). White bars, wakefulness; dashed bars, NREM sleep; black bars, REM sleep. (B) discharge pattern of individual NREM/REM sleep-related VLPO neuron recorded across sleep–wake states in WAG/Rij rat. The cell exhibited NREM sleep/W ratio >2 and more than 3 fold increase in their firing during REM sleep vs. W Note that the cell fired at maximal rate at sleep onset and gradually decreased discharge during NREM sleep episodes. Expanded tracings from the sections marked by horizontal bars show neuronal discharge during waking (b_1), NREM sleep (b_2) and REM sleep (b_3). *$p<0.05$; ⁂$p<0.01$; ⁂$p<0.001$, Tukey's *post-hoc* test.

related neurons between WAG/Rij and non-epileptic Sprague–Dawley rats ($p>0.05$). No W-related cells were recorded in WAG/Rij as well as in non-epileptic rats.

Within the VLPO, the percentage of W/REM sleep-related cells and W-related cells in WAG/Rij rats (21.9% and 31.3%, respectively, Fig. 6*A*) was higher than in non-epileptic rats (14.6% and 17.1%, respectively). Strain differences in firing rates of both W/REM sleep-related and W-related neurons were insignificant ($p>0.05$, two-way repeated measures ANOVA).

State-indifferent neurons

The cells belonging to this group did not exhibit significant state-dependent changes in the mean firing rate.

Within the MnPN and VLPO, percentages of state-indifferent neurons in WAG/Rij rats (43.2% and 28.1%, respectively) were higher than in non-epileptic Sprague–Dawley rats (11.2% and 12.2%, respectively) (Figs. 5A, B and 6A). MnPN state-indifferent neurons discharged at lower rates in WAG/Rij compared to Sprague–Dawley rats across all examined sleep–wake states ($F_{(1,\ 49)} = 85.5$, $p<0.001$), whereas strain differences in discharge of VLPO state-indifferent cells were not significant.

Experiments 4 and 5: induction of primary generalized seizures in non-epileptic rats using electrical stimulation and chemical manipulations of the MnPN

Electrical stimulation

Electrical stimulation of the MnPN in non-epileptic Sprague–Dawley rats triggered primary generalized seizures in a state-dependent manner.

During active and quiet waking with irregular low-amplitude (desynchronized) EEG activity trains of stimuli consisting of 200 μs, 150–200 μA square pulses at 8–13 pulses/s provoked absence-like seizures on the first trial. At the beginning, stimulation induced almost immediate arrest of ongoing behavior along with 1–2 s in duration bilateral waxing and waning surface-negative responses in frontal and parietal cortices (Fig. 7A). The amplitude of evoked rhythmic EEG activity was comparable with that of spontaneous thalamocortical oscillations characteristic of quite waking (sensorimotor rhythm) and NREM sleep (sleep spindles). Evoked responses resembling SWDs appeared with 4.6 ± 0.5 s latency, lasted 4.3 ± 0.6 s, and were accompanied by immobility, staring and twitching of whiskers. Primary afterdischarge was represented by generalized polyspike-wave and spike-wave 5–9 Hz activity that lasted for 34.6 ± 1.2 s. During the course of afterdischarge, periods of immobility alternated with scanning head movements involving extension of the neck or intensive face washing. Secondary (recurrent) afterdischarge started 49.8 ± 3.7 s after termination of the primary afterdischarge, consisted of bilateral waxing polyspike-wave complexes at 1–2 Hz, lasted for 22.6 ± 2.8 s, and was accompanied by rearing against the wall of the cage. Repetitive induction of seizures caused an increase in duration and waveform complexity of the primary and secondary afterdischarge (Fig. 8A). All gradually evolving motor manifestations of the seizure (chewing, head nodding, bilateral limb clonus, tonic–clonic convulsions) occurred during the secondary afterdischarge. The first generalized tonic–clonic seizure appeared during 10th–14th seizure induction. During tonic–clonic seizure EEG was represented by continuous spikes and waves with waxing amplitude and decreasing frequency (from 5–6 Hz to 2–3 Hz) during seizure progression (Fig. 8A).

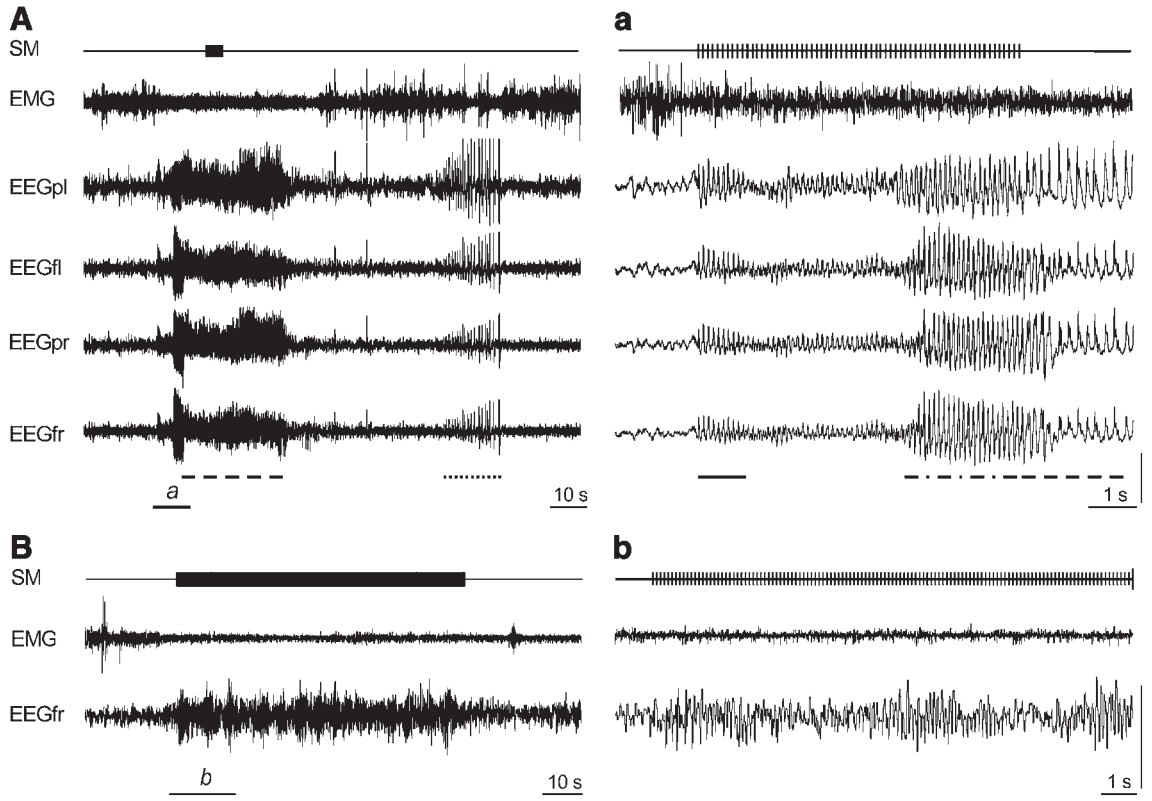

Fig. 7. (A) induction of the first primary generalized non-convulsive seizure in waking in response to low-frequency stimulation of the MnPN. a, expanded tracing from A marked by horizontal bar. Note that stimulation immediately induced behavioral arrest along with waxing and waning responses (indicated by solid line under the EEG tracing in *a*). SWDs (marked with dashed and dotted line in a) were accompanied by behavioral manifestations typical for absence seizures. Both primary (dashed lines in A and a) and secondary (dotted line in A) afterdischarges appeared bilaterally in frontal and parietal EEG and were represented by polyspike-wave and spike-wave discharges. (B) effects of low-frequency stimulation of the MnPN in NREM sleep. Note that stimulation induces waxing and waning responses. SM, stimulation mark; EMG, electromyogram; EEGfr, EEGfl, EEGpr, and EEGpl, electroencephalogram recorded from frontal right, frontal left, parietal right, and parietal left cortices. Vertical bar, 500 μV.

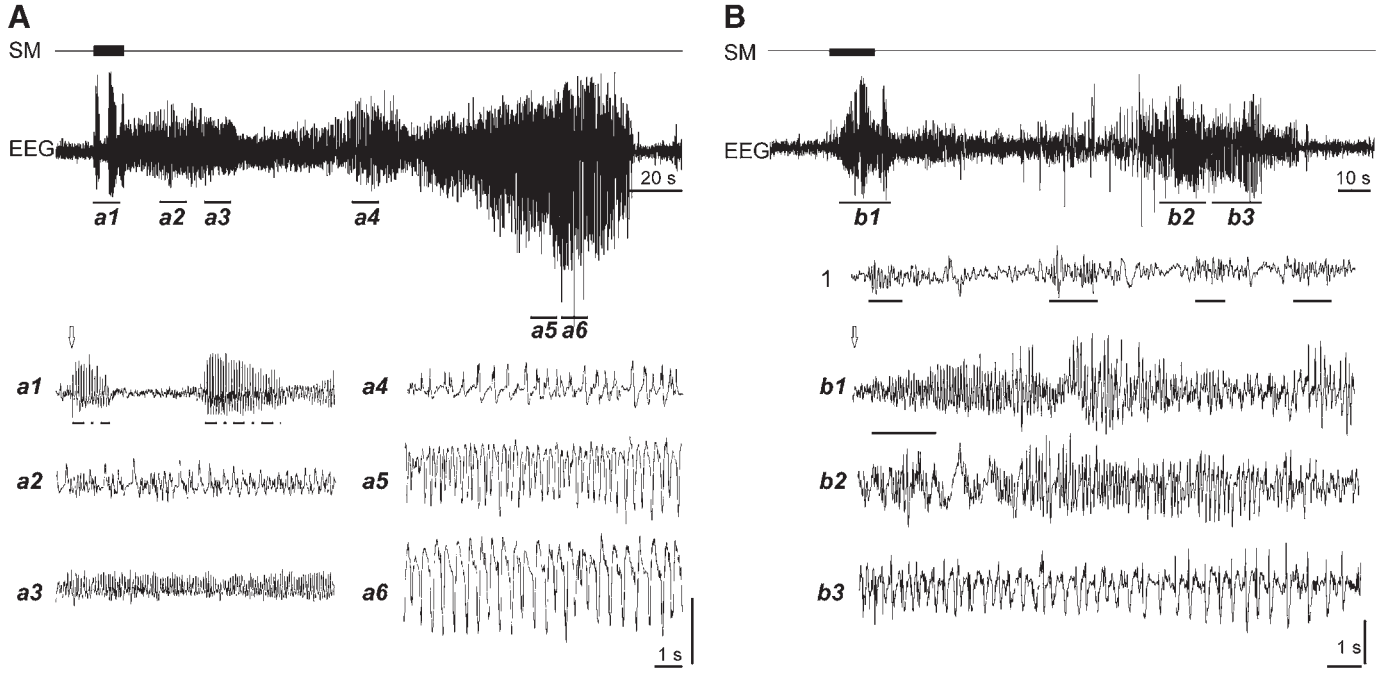

Fig. 8. (A), Induction of first generalized tonic–clonic seizure by low-frequency (10 Hz) stimulation of the MnPN (seizure #12 from the beginning of kindling). *a1–6*, expanded EEG tracings. Tracings *a5* and *a6* correspond to tonic–clonic seizure. Note that stimulation first induces a series of absence-like paroxysms (indicated by dashed and dotted lines under the EEG tracing in *a1*) and increased complexity of the waveforms constituting afterdischarges. (B) Induction of generalized seizure by high-frequency (100 Hz) stimulation of the MnPN. *b1–3*, expanded EEG tracings. *b1*, absence-like seizure. Note that stimulation first evoked rhythmic activity resembling sleep spindles (indicated by solid lines in *1* and *b1*) that progressively grows in amplitude and transforms to SWDs with amplitude–frequency characteristics similar to that in genetic absence epilepsy rats. *b2–3*, seizure with motor components (jar clonus, head nodding, bilateral forelimb clonus). *1*— EEG during NREM sleep. Arrows indicate the beginning of stimulation. SM, stimulation mark, EEG, electroencephalogram. Vertical bars, 1.5 mV (A) and 0.5 mV (B).

In three out of five animals repetitive induction of seizures did not affect the initial EEG response to stimulation resembling normal rhythmic EEG activity. In two animals, following induction of 3–5 seizures, first stimuli applied to the MnPN induced SWDs (Fig. 8A).

An increase in the duration of stimulation resulted in sequential appearance of 3–4 short-lasting (1.5–4 s) SWDs prior to emergence of the other paroxysmal waveforms and abnormal behavioral manifestations.

During active waking accompanied by vigorous exploratory activity and theta rhythm in the parietal EEG, stimulation with the same parameters induced immobility along with constant amplitude responses in the EEG with voltage 1.5–2 fold higher than that of background EEG. Following 8–10 s these responses were transformed into SWDs.

During sleep stimulation adequate to induce SWDs during waking did not evoke abnormal patterns of EEG activity. Spindle-like activity was induced during NREM sleep (Fig. 7B) and constant low-amplitude responses in REM sleep. An increase in the duration of stimulation during sleep did not result in seizure induction (Fig. 7B). An increase in the stimulation intensity also was ineffective until the point when current reached the threshold for awakening (600–800 μA); arousal was followed by seizure in a few seconds.

High-frequency (100 Hz, 200 μA) stimulation of the MnPN in waking caused almost immediate behavioral arrest in parallel with appearance of 12–14 Hz rhythmic EEG activity which amplitude was comparable to that of sleep spindles for 1.5–2 s (Fig. 8B). During subsequent 4–5 s rhythmic oscillations exhibited progressive 3–4 fold increase in amplitude along with decline in frequency to about 8–10 Hz. SWDs were accompanied by behavioral correlates of absence seizures. The subsequent behavioral and EEG manifestations of seizure were very similar to those evoked by low-frequency stimulation except presence of high-amplitude slow waves with superimposed spikes during primary and secondary afterdischarges. During NREM sleep evoked EEG activity resembled spindling. In REM sleep stimulation induced oscillations within the same frequency range as during NREM sleep but with constant amplitude that did not exceed the amplitude of background activity.

Normal and pathological EEG-synchronizing responses induced by low- and high-frequency stimulation of the MnPN were site-specific. If stimulating electrodes were localized 150–200 μm lateral to the MnPN, stimulation resulted in failure to evoke the same EEG patterns.

Chemical manipulations

The major limitation of the method of electrical stimulation is lack of selectivity for neurons. Given that a possible role of activation of passing fibers and/or axonal terminals could not be ruled out, we applied local chemical activation and inhibition of neuronal cell bodies and dendrites within the MnPN.

Microdialytic perfusion of the MnPN in non-epileptic rats with 1 mM glutamate, 50 μM bicuculline and 50 μM muscimol did not cause any EEG abnormalities. However, L-glutamate and bicuculline at 10 mM and 100 μM concentrations, respectively, induced short (1.5–3.5 s) multiple 6–8 Hz SWDs with waxing and waning amplitude accompanied by transient immobility, staring and twitching of vibrissae. These paroxysms appeared during prolonged period of fluctuating vigilance between AW and light NREM sleep. SWDs were timed to periods of quiet waking, which often were followed by short (8–40 s) episodes of light NREM sleep (Fig. 9A). MnPN perfusion with 100 μM muscimol for 15 min caused a hyperactive state that lasted for 0.5–1.5 h. The first attempts of falling asleep following this period were also accompanied by multiple SWDs with similar characteristics to those induced by glutamate and bicuculline perfusion (Fig. 9B).

Discussion

In 1981 Halasz suggested that AE is a "…disorder of the function of sleep promotion" based on assumption that SWDs are epileptic variation of K-complexes, considered as "building stones" of the process of falling asleep due to their presumed sleep-promoting effect. In this study we obtained new evidence for the hypothesis that AE is a

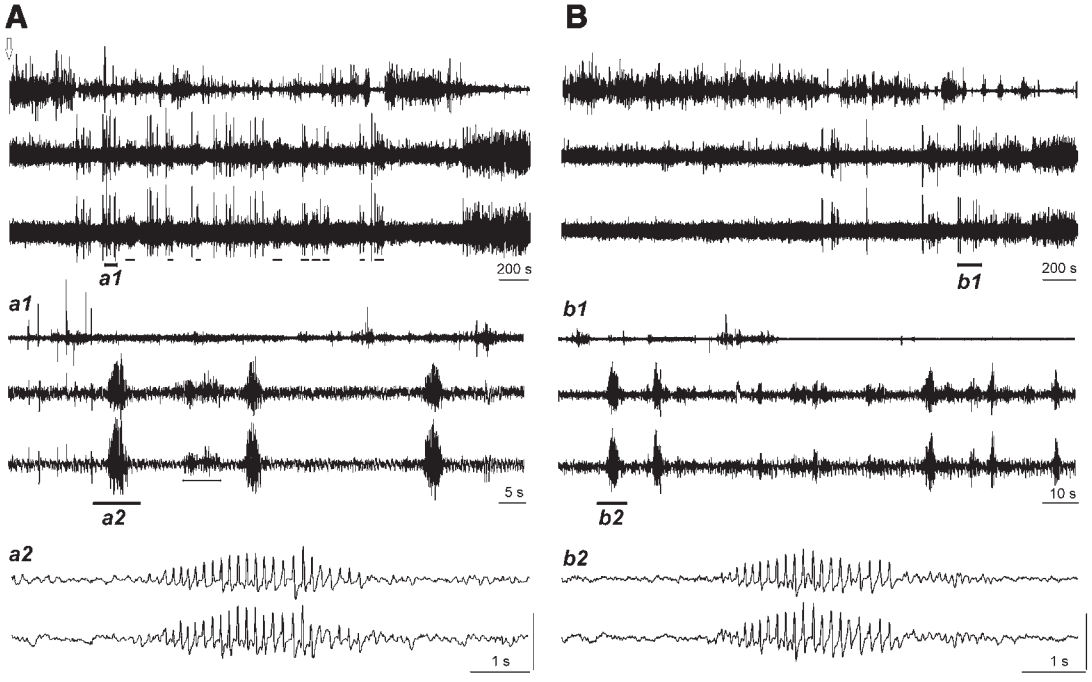

Fig. 9. Induction of absence-like seizures by microdialytic perfusion of the MnPN with 10 mM L-glutamate (A) and 100 μM muscimol (B). a1, b1, expanded tracings from A and B, respectively, marked by horizontal bars. a2, b2, expanded tracings from a1 and b1 marked by horizontal bars depicting SWDs morphology. Arrow in A indicates the start of L-glutamate perfusion. Polygraphic recording shown in B starts 20 min after termination of muscimol perfusion. Note that during L-glutamate perfusion SWDs are timed to episodes of quiet waking often followed by light NREM sleep episodes (indicated by solid lines in A and a1). In response to muscimol perfusion, SWDs appear after prolonged hyperarousal during first attempts of falling asleep. Vertical bar, 0.4 mV.

disorder of a sleep-promoting function. We found insufficiency of the preoptic sleep-promoting mechanisms in WAG/Rij rats, an established model of human absence epilepsy. WAG/Rij rats lacked sleep-associated c-Fos activation of GABAergic neurons in the MnPN and VLPO and exhibited lower numbers and % GABAergic neurons expressing c-Fos in sleeping condition, compared to non-epileptic Wistar and ACI rats. WAG/Rij rats also exhibited a lower percentage of neurons that increased their discharge during sleep in the MnPN and VLPO, and reduced firing rates of sleep-active MnPN cells. We also found that incomplete activation of the sleep-promoting mechanisms during waking using electrical stimulation and chemical manipulations restricted to the MnPN site was sufficient to induce absence-like seizures in non-epileptic rats. We hypothesize that deficiency of the preoptic sleep-promoting system with inadequate suppression of arousal systems on transition to sleep may play an important role in pathogenesis of non-convulsive seizures resembling human absences in WAG/Rij rats.

The presence of sleep-active GABA/galaninergic neuronal populations within the VLPO and MnPN was initially discovered in non-epileptic Sprague–Dawley rats using c-Fos expression as a marker of neuronal activation (Sherin et al., 1996, 1998; Gong et al., 2000, 2004; Gaus et al., 2002). In agreement with these studies, both sleeping vs. sleep-deprived Wistar rats and sleeping vs. spontaneously awake ACI rats exhibited higher total c-Fos immunoreactivity within the rostral MnPN and higher c-Fos activation of GABAergic neurons within the MnPN and VLPO cluster. However, Wistar and ACI rats did not exhibit sleep-associated increases in total c-Fos immunoreactivity within the VLPO cluster as found in Sprague–Dawley rats (Sherin et al., 1996; Gong et al., 2004; Gvilia et al., 2006). Our findings are consistent with those of Modirrousta et al. (2004) in Wistar rats, including the absence of increase in the total c-Fos expression within the VLPO cluster and activation of GABAergic neurons within the VLPO cluster and MnPN during sleep compared to sleep deprivation. Therefore, in all three strains of non-epileptic rats studied to-date immunohistochemical studies revealed sleep-related increases in total c-Fos immunoreactivity within the MnPN and sleep-associated activation of GABAergic neurons within the VLPO cluster and MnPN.

WAG/Rij rats did not differ from non-epileptic rats in MnPN and VLPO c-Fos expression during enforced or spontaneous waking. However, during sleep, compared to waking, WAG/Rij rats did not exhibit increases in total number of c-Fos$^+$ cells and c-Fos$^+$/GAD$^+$ neurons within the MnPN, VLPO cluster and medial extended VLPO found in non-epileptic rats. As a result, in sleeping condition within each of these sites, total c-Fos expression and/or c-Fos activation of GAD$^+$ cells in WAG/Rij rats was lower than in non-epileptic animals. Within the dorsal extended VLPO, both non-epileptic and WAG/Rij rats exhibited a decrease in total c-Fos immunoreactivity and/or in c-Fos activation of GABAergic neurons during sleep compared to sleep deprivation or spontaneous waking.

Although we were unable to identify sleep-active neuronal groups within the VLPO and MnPN in WAG/Rij rats using c-Fos immunohistochemistry, our electrophysiological studies revealed the presence of sleep-related cells within these sites. However, within the VLPO, the percent sleep-active cells was a third of that in non-epileptic Sprague–Dawley rats (Szymusiak et al., 1998). In the MnPN, the percent NREM/REM sleep-related cells within the sample recorded was a 2.6 times lower compared to Sprague–Dawley rats (Suntsova et al., 2002). Within each group of sleep-related MnPN cells, the mean firing rates during the states with the maximal discharge were 20–40% of those in non-epileptic rats. The differences in VLPO and MnPN neuronal discharge between WAG/Rij and non-epileptic rats provide possible explanations for the failure to identify sleep-active neuronal groups in WAG/Rij rats using c-Fos immunohistochemistry. First, due to significantly reduced number of cells with sleep-associated discharge profile in WAG/Rij rats, the number of GABAergic neurons expressing c-Fos during sleep and during waking could be comparable, so a distinct sleep-active population would not be recognized. Second, increased neuronal firing is not always associated with c-Fos expression (Hoffman and Lyo, 2002). Immediate early gene *c-fos* is transcriptionally activated by membrane depolarization (Sheng et al., 1990). Given that in WAG/Rij, compared to non-epileptic rats, sleep-related MnPN neurons discharged at lower rates, it is possible that in WAG/Rij rats depolarization of some cells during sleep did not reach the level triggering *c-fos* induction.

In agreement with previously published data (van Luijtelaar and Coenen, 1988; Drinkenburg et al., 1995), WAG/Rij rats had lower numbers of SWDs in sleeping vs. sleep-deprived and spontaneously predominantly awake conditions. The difference in the number of seizures between the conditions could not account for the absence of sleep-associated increase in c-Fos immunoreactivity within the MnPN and VLPO in WAG/Rij rats. During SWDs sleep-active MnPN and VLPO neurons exhibit a phasic, approximately 5 s in duration decrease of discharge (Suntsova et al., 2006). The inhibitory impact of SWDs on activity of sleep-related neurons was the lowest in sleeping condition. We calculated that the total duration of decrease in discharge resulting from SWDs in sleeping and spontaneously awake/sleep-deprived conditions was less than 1 and 2 min, respectively, out of 2 h of recording.

The reduced c-Fos expression in a population of GABAergic neurons, lower number and discharge of sleep-related cells within the VLPO and MnPN found in WAG/Rij rats may result from pathological impairments within the sleep-promoting system itself. In favor of this hypothesis, WAG/Rij rats exhibited relatively mild (20–25%) but statistically significant ($p<0.01$, Student's *T*-test) reductions in the number of GABAergic cells within the VLPO cluster and the rostral MnPN compared to Wistar and ACI rats, respectively. Partial loss of GABAergic sleep-promoting neurons may lead to insufficient inhibition of one or several components of arousal system, which, in turn, may result in stronger inhibitory control over the intact sleep-active cells causing reductions in their firing rates seen in WAG/Rij rats. However, only a subset of GABAergic neurons within the VLPO and MnPN are sleep-active and, therefore there is no certainty that the number of GABAergic cells in WAG/Rij rats is reduced due to loss of sleep-active neurons. The other possibility is that primary hyperactivity of one or several waking-promoting neuronal groups known to exercise inhibitory control over preoptic sleep-promoting neurons (Gallopin et al., 2000) causes functional inhibition of sleep-active MnPN and VLPO neurons.

The major abnormalities in sleep architecture found in WAG/Rij rats include difficulties in falling asleep and prolonged NREM/REM sleep transitions, often followed by arousals (Gandolfo et al., 1990; Coenen and van Luijtelaar, 2003; van Luijtelaar and Bikbaev, 2007). This suggests that deficiencies in MnPN and VLPO sleep-active neurons we found lead to deficits in control of transitions from waking to sleep and from NREM to REM sleep. The fact that majority of NREM/REM sleep-related cells have peak discharge during transitions to NREM and REM sleep (see Fig. 7) favors an important role of these cells in mechanisms underlying initiation of NREM and REM sleep states.

We hypothesize that idiopathic deficiency of preoptic sleep-promoting mechanisms can make transitional sleep–wake states seizure-prone due to altered, unequal inhibitory control over multiple arousal neuronal groups. Ineffective inhibition of one or several components of the arousal system may lead to imbalance in the ascending control of the thalamocortical circuitry, which has been suggested as one of the pathogenic mechanisms underlying SWDs generation (Snead, 1995; Danober et al., 1998). In agreement with our hypothesis, the incidence of SWDs in WAG/Rij rats is the lowest at the beginning of the light phase, when the sleep pressure is at its maximum, and increases at the end of the light phase (van Luijtelaar and Coenen, 1988; van Luijtelaar and Bikbaev, 2007). Potentiation of the process of falling asleep by using benzodiazepine and

imidazopyridine hypnotics is known to cause reductions in the number and duration of SWDs in WAG/Rij rats (Marescaux et al., 1985; Depoortere et al., 1995). In this study we simulated deficiency of the sleep-promoting mechanisms by activation or inhibition of one component the sleep-promoting neuronal population. Electrical stimulation and chemical manipulations were restricted to the MnPN site and did not affect the other sleep-promoting neuronal groups directly. We found that activation of the MnPN during waking, while insufficient to cause the complete suppression of arousal systems required for initiation of sustained sleep, induced absence-like seizures in non-epileptic rats. Both low- and high-frequency stimulation of the MnPN evoked 8–14 Hz rhythmic activity resembling normal thalamocortical oscillations followed by SWDs with amplitude–frequency characteristics similar to those in genetic absence epilepsy rats. SWDs were accompanied by behavioral manifestations typical for absence seizures. With repetitive inductions, seizures rapidly progressed to generalized tonic–clonic seizures. However, all induced paroxysms started as absences, the changes in EEG and motor manifestations caused by kindling were mainly timed to the secondary afterdischarge. During sleep, when activity of the entire sleep-active neuronal population is high, stimulation with the same intensity failed to trigger SWDs. An increase in current intensity was ineffective until it reached the threshold for awakening, which likely resulted from spread of current to adjacent structures. The effects of chemical manipulations of the MnPN were in accordance with effects of electrical stimulation. L-glutamate and bicuculline perfusion in the dark phase induced multiple absence-like seizures during periods of quiet waking. We hypothesize that partial activation of sleep-promoting system during spontaneous wake being insufficient for sleep initiation induced a pathological state of decreased vigilance characterized by unequal inhibition of wake-promoting neuronal groups, and imbalance in the ascending control of thalamocortical system. Note, that activation of subset of sleep-promoting neurons located within the VLPO by glutamate microinjection also triggered SWDs (J. Lu, personal communications). The results of stimulation experiments cannot solely demonstrate the causative link between insufficient inhibitory control over the arousal neuronal groups and absence seizures, because the existence of alternative, currently unknown mechanism leading to SWDs in response to activation of MnPN neurons cannot be excluded. However, the results of chemical inhibition experiments provide further evidence supporting the role of insufficiency of sleep-promoting mechanisms in SWDs induction. Perfusion of the MnPN with muscimol during the light phase caused absence-like seizures during the first attempts of falling asleep as the prolonged muscimol-induced hyperarousal response is subsiding. In this case the driving source of absence seizures could be residual inhibition of some sleep-promoting MnPN neurons causing insufficiency of homeostatically activated sleep-promoting mechanisms and abnormal ascending control of thalamocortical circuitry.

The effects of chemical manipulations of the MnPN are in line with the effects of more localized electrical stimulation and effects of both interventions are in agreement with the data on insufficiency of the sleep-promoting mechanisms in genetic absence epilepsy WAG/Rij rats. However, the possibility of involvement of cells in adjacent preoptic area/basal forebrain subregions during experimental manipulations of MnPN activity should be taken into account. Our results suggest that local chemical manipulation of neuronal activity within preoptic area/basal forebrain is sufficient to induce absence paroxysms.

Although further studies are needed to clarify whether abnormal functioning of sleep–wake-generating circuitry on wake-sleep transitions underlies or contributes to genesis of absence-like seizures, preoptic GABA/galaninergic sleep-promoting neuronal groups can be considered as potential targets for pharmacological and behavioral interventions in AE. Independently of the primary pathology underlying absence phenotype, AE patients exhibiting difficulties with sleep initiation and maintenance would benefit from improved sleep architecture. Potentiation of the sleep-promoting mechanisms by short-acting hypnotics administered at night time and/or strict sleep hygiene may reduce the incidence of SWDs due to optimization of the ascending control over the thalamocortical excitability, reduction in the duration of the seizure-prone transitional states and in the number of seizure-associated deviant arousals (Niedermeyer, 1996). Improved sleep efficiency would reduce the daytime sleepiness, common in AE (Maganti et al., 2006, Byars et al., 2008), and, therefore, the frequency of absence seizures, which mostly occur during episodes of decreased or fluctuating vigilance (Crunelli and Leresche, 2002).

Acknowledgments

This research was supported by the Medical Research Service of the Department of Veterans Affairs, NIH grants MH075076, HL60296, NS-50939 and the J. Christian Gillin Research Grant from the Sleep Research Society Foundation (N.S.) We thank Dr. M.N. Shouse for helpful comments on the work and Keng-Tee Chew for technical assistance.

References

Avanzini, G., de, C.M., Franceschetti, S., Sancini, G., Spreafico, R., 1996. Cortical versus thalamic mechanisms underlying spike and wave discharges in GAERS. Epilepsy Res. 26, 37–44.
Baldy-Moulinier, M., 1992. Sleep architecture and childhood absence epilepsy. Epilepsy Res. Suppl. 6, 195–198.
Barreto, J.R., Fernandes, R.M., Sakamoto, A.C., 2002. Correlation of sleep macrostructure parameters and idiopathic epilepsies. Arq. Neuro-Psiquiatr. 60, 353–357.
Broicher, T., Kanyshkova, T., Meuth, P., Pape, H.C., Budde, T., 2008. Correlation of T-channel coding gene expression, IT, and the low threshold Ca2+ spike in the thalamus of a rat model of absence epilepsy. Mol. Cell Neurosci. 39, 384–399.
Budde, T., Caputi, L., Kanyshkova, T., Staak, R., Abrahamczik, C., Munsch, T., Pape, H.C., 2005. Impaired regulation of thalamic pacemaker channels through an imbalance of subunit expression in absence epilepsy. J. Neurosci. 25, 9871–9882.
Byars, A.W., Byars, K.C., Johnson, C.S., DeGrauw, T.J., Fastenau, P.S., Perkins, S., Austin, J.K., Dunn, D.W., 2008. The relationship between sleep problems and neuropsychological functioning in children with first recognized seizures. Epilepsy Behav. 13, 607–613.
Coenen, A.M., van Luijtelaar, E.L., 2003. Genetic animal models for absence epilepsy: a review of the WAG/Rij strain of rats. Behav. Genet. 33, 635–655.
Crunelli, V., Leresche, N., 2002. Childhood absence epilepsy: genes, channels, neurons and networks. Nat. Rev. Neurosci. 3, 371–382.
D'Antuono, M., Inaba, Y., Biagini, G., D'Arcangelo, G., Tancredi, V., Avoli, M., 2006. Synaptic hyperexcitability of deep layer neocortical cells in a genetic model of absence seizures. Genes Brain Behav. 5, 73–84.
Danober, L., Deransart, C., Depaulis, A., Vergnes, M., Marescaux, C., 1998. Pathophysiological mechanisms of genetic absence epilepsy in the rat. Prog. Neurobiol. 55, 27–57.
Depoortere, H., Francon, D., van Luijtelaar, E.L., Drinkenburg, W.H., Coenen, A.M., 1995. Differential effects of midazolam and zolpidem on sleep–wake states and epileptic activity in WAG/Rij rats. Pharmacol. Biochem. Behav. 51, 571–576.
Drinkenburg, W.H., Coenen, A.M., Vossen, J.M., van Luijtelaar, E.L., 1995. Sleep deprivation and spike-wave discharges in epileptic rats. Sleep 18, 252–256.
Gallopin, T., Fort, P., Eggermann, E., Cauli, B., Luppi, P.H., Rossier, J., Audinat, E., Muhlethaler, M., 2000. M.Serafin, Identification of sleep-promoting neurons in vitro. Nature 404, 992–995.
Gandolfo, G., Romettino, S., Gottesmann, C., van, L.G., Coenen, A., 1990. Genetically epileptic rats show a pronounced intermediate stage of sleep. Physiol. Behav. 47, 213–215.
Gaus, S.E., Strecker, R.E., Tate, B.A., Parker, R.A., Saper, C.B., 2002. Ventrolateral preoptic nucleus contains sleep-active, galaninergic neurons in multiple mammalian species. Neuroscience 115, 285–294.
Gloor, P., Fariello, R.G., 1988. Generalized epilepsy: some of its cellular mechanisms differ from those of focal epilepsy. Trends Neurosci. 11, 63–68.
Gong, H., Szymusiak, R., King, J., Steininger, T., McGinty, D., 2000. Sleep-related c-Fos protein expression in the preoptic hypothalamus: effects of ambient warming. Am. J. Physiol Regul. Integr. Comp. Physiol. 279, R2079–R2088.
Gong, H., McGinty, D., Guzman-Marin, R., Chew, K.T., Stewart, D., Szymusiak, R., 2004. Activation of c-fos in GABAergic neurones in the preoptic area during sleep and in response to sleep deprivation. J. Physiol. 556, 935–946.
Govindaiah, G., Cox, C.L., 2006. Modulation of thalamic neuron excitability by orexins. Neuropharmacology 51, 414–425.
Gvilia, I., Xu, F., McGinty, D., Szymusiak, R., 2006. Homeostatic regulation of sleep: a role for preoptic area neurons. J. Neurosci. 26, 9426–9433.
Halasz, P., 1981. Generalized epilepsy with spike-wave paroxysms as an epileptic disorder of the function of sleep promotion. Acta Physiol. Acad. Sci. Hung. 57, 51–86.

Halasz, P., Terzano, M.G., Parrino, L., 2002. Spike-wave discharge and the microstructure of sleep–wake continuum in idiopathic generalised epilepsy. Neurophysiol. Clin. 32, 38–53.
Hoffman, G.E., Lyo, D., 2002. Anatomical markers of activity in neuroendocrine systems: are we all 'fos-ed out'? J. Neuroendocrinol. 14, 259–268.
Hosford, D.A., Wang, Y., Cao, Z., 1997. Differential effects mediated by GABAA receptors in thalamic nuclei in lh/lh model of absence seizures. Epilepsy Res. 27, 55–65.
Huang, J., Mai, J.N., Wang, X.Y., Li, Z.B., Zhang, F.Q., 2007. [Overnight sleep structure of children with epilepsia.]. Zhongguo Dang. Dai Er. Ke. Za Zhi. 9, 6–10.
Huguenard, J.R., McCormick, D.A., 2007. Thalamic synchrony and dynamic regulation of global forebrain oscillations. Trends Neurosci. 30, 350–356.
Inoue, M., Peeters, B.W., van Luijtelaar, E.L., Vossen, J.M., Coenen, A.M., 1990. Spontaneous occurrence of spike-wave discharges in five inbred strains of rats. Physiol. Behav. 48, 199–201.
Kole, M.H., Brauer, A.U., Stuart, G.J., 2007. Inherited cortical HCN1 channel loss amplifies dendritic calcium electrogenesis and burst firing in a rat absence epilepsy model. J. Physiol. 578, 507–525.
Lu, J., Bjorkum, A.A., Xu, M., Gaus, S.E., Shiromani, P.J., Saper, C.B., 2002. Selective activation of the extended ventrolateral preoptic nucleus during rapid eye movement sleep. J. Neurosci. 22, 4568–4576.
Luhmann, H.J., Mittmann, T., van, L.G., Heinemann, U., 1995. Impairment of intracortical GABAergic inhibition in a rat model of absence epilepsy. Epilepsy Res. 22, 43–51.
Maganti, R., Sheth, R.D., Hermann, B.P., Weber, S., Gidal, B.E., Fine, J., 2005. Sleep architecture in children with idiopathic generalized epilepsy. Epilepsia 46, 104–109.
Maganti, R., Hausman, N., Koehn, M., Sandok, E., Glurich, I., Mukesh, B.N., 2006. Excessive daytime sleepiness and sleep complaints among children with epilepsy. Epilepsy Behav. 8, 272–277.
Marescaux, C., Micheletti, G., Vergnes, M., Rumbach, L., Warter, J.M., 1985. Diazepam antagonizes GABAmimetics in rats with spontaneous petit mal-like epilepsy. Eur. J. Pharmacol. 113, 19–24.
McCormick, D.A., 1992. Neurotransmitter actions in the thalamus and cerebral cortex and their role in neuromodulation of thalamocortical activity. Prog. Neurobiol. 39, 337–388.
Merlo, D., Mollinari, C., Inaba, Y., Cardinale, A., Rinaldi, A.M., D'Antuono, M., D'Arcangelo, G., Tancredi, V., Ragsdale, D., Avoli, M., 2007. Reduced GABAB receptor subunit expression and paired-pulse depression in a genetic model of absence seizures. Neurobiol. Dis. 25, 631–641.
Modirrousta, M., Mainville, L., Jones, B.E., 2004. Gabaergic neurons with alpha2-adrenergic receptors in basal forebrain and preoptic area express c-Fos during sleep. Neuroscience 129, 803–810.
Niedermeyer, E., 1996. Primary (idiopathic) generalized epilepsy and underlying mechanisms. Clin. Electroencephalogr. 27, 1–21.
Paxinos, G., Watson, C., 1998. The Rat Brain in Stereotaxic Coordinates, fourth ed. Academic Press, San Diego, London.
Pumain, R., Louvel, J., Gastard, M., Kurcewicz, I., Vergnes, M., 1992. Responses to N-methyl-D-aspartate are enhanced in rats with petit mal-like seizures. J. Neural Transm. Suppl. 35, 97–108.
Saper, C.B., Chou, T.C., Scammell, T.E., 2001. The sleep switch: hypothalamic control of sleep and wakefulness. Trends Neurosci. 24, 726–731.
Sheng, M., McFadden, G., Greenberg, M.E., 1990. Membrane depolarization and calcium induce c-fos transcription via phosphorylation of transcription factor CREB. Neuron 4, 571–582.
Sherin, J.E., Shiromani, P.J., McCarley, R.W., Saper, C.B., 1996. Activation of ventrolateral preoptic neurons during sleep. Science 271, 216–219.
Sherin, J.E., Elmquist, J.K., Torrealba, F., Saper, C.B., 1998. Innervation of histaminergic tuberomammillary neurons by GABAergic and galaninergic neurons in the ventrolateral preoptic nucleus of the rat. J. Neurosci. 18, 4705–4721.
Snead, O.C., 1995. Basic mechanisms of generalized absence seizures. Ann. Neurol. 37, 146–157.
Steriade, M., 1999. Brainstem activation of thalamocortical systems. Brain Res. Bull. 50, 391–392.
Strauss, U., Kole, M.H., Brauer, A.U., Pahnke, J., Bajorat, R., Rolfs, A., Nitsch, R., Deisz, R.A., 2004. An impaired neocortical Ih is associated with enhanced excitability and absence epileps. Eur. J. Neurosci. 19, 3048–3058.
Sun, S.Z., Wang, M.W., Feng, Z.H., Zhang, F.Z., Shi, R.F., 2005. [Relationship between idiopathic epilepsy and sleep macrostructure in children]. Di Yi. Jun. Yi. Da. Xue. Xue. Bao. 25, 354–356.
Suntsova, N., Szymusiak, R., Alam, M.N., Guzman-Marin, R., McGinty, D., 2002. Sleep-waking discharge patterns of median preoptic nucleus neurons in rats. J. Physiol. 543, 665–677.
Suntsova, N., Kumar, S., Guzman-Marin, R., Shouse, M., Szymusiak, R., McGinty, D., 2006. Absence epilepsy and the hypothalamic sleep-promoting and arousal systems. J. Sleep Res. 15, 220.
Suntsova, N., Guzman-Marin, R., Kumar, S., Alam, M.N., Szymusiak, R., McGinty, D., 2007. The median preoptic nucleus reciprocally modulates activity of arousal-related and sleep-related neurons in the perifornical lateral hypothalamus. J. Neurosci. 27, 1616–1630.
Swanson, L.W., 1998. Brain Maps: Structure of the Rat Brain, second ed. Elsevier, Amsterdam.
Szymusiak, R., Alam, N., Steininger, T.L., McGinty, D., 1998. Sleep-waking discharge patterns of ventrolateral preoptic/anterior hypothalamic neurons in rats. Brain Res. 803, 178–188.
Szymusiak, R., McGinty, D., 2008. Hypothalamic regulation of sleep and arousal. Ann. N. Y. Acad. Sci. 1129, 275–286.
Talley, E.M., Solorzano, G., Depaulis, A., Perez-Reyes, E., Bayliss, D.A., 2000. Low-voltage-activated calcium channel subunit expression in a genetic model of absence epilepsy in the rat. Brain Res. Mol. Brain Res. 75, 159–165.
Tan, H.O., Reid, C.A., Chiu, C., Jones, M.V., Petrou, S., 2008. Increased thalamic inhibition in the absence seizure prone DBA/2J mouse. Epilepsia 49, 921–925.
Timo-Iaria, C., Negrao, N., Schmidek, W.R., Hoshino, K., Lobato de Menezes, C.E., Leme da Rocha, T., 1970. Phases and states of sleep in the rat. Physiol. Behav. 5, 1057–1062.
Tybout, A., Sternthal, B, 2001. Can I test for simple effects in the presence of an insignificant interaction? J. Consum. Psychol. 10, 5–10.
van de Bovenkamp-Janssen, M.C., Akhmadeev, A., Kalimullina, L., Nagaeva, D.V., van Luijtelaar, E.L., Roubos, E.W., 2004. Synaptology of the rostral reticular thalamic nucleus of absence epileptic WAG/Rij rats. Neurosci. Res. 48, 21–31.
van Luijtelaar, E.L., Coenen, A.M., 1986. Two types of electrocortical paroxysms in an inbred strain of rats. Neurosci. Lett. 70, 393–397.
van Luijtelaar, E.L., Coenen, A.M., 1988. Circadian rhythmicity in absence epilepsy in rats. Epilepsy Res. 2, 331–336.
van Luijtelaar, G., Bikbaev, A., 2007. Midfrequency cortico-thalamic oscillations and the sleep cycle: genetic, time of day and age effects. Epilepsy Res. 73, 259–265.
van Luijtelaar, G., Sitnikova, E., 2006. Global and focal aspects of absence epilepsy: the contribution of genetic models. Neurosci. Biobehav. Rev. 30, 983–1003.